11-13-2015

Species Specific Microcalcification in Reef Building Caribbean Corals in Ocean Acidification Conditions

Ashley M. Dungan

Nova Southeastern University, ad1211@nova.edu

This document is a product of extensive research conducted at the Nova Southeastern University Halmos College of Natural Sciences and Oceanography. For more information on research and degree programs at the NSU Halmos College of Natural Sciences and Oceanography, please click here.

Follow this and additional works at: http://nsuworks.nova.edu/occ_stuetd

Part of the Marine Biology Commons, and the Oceanography and Atmospheric Sciences and Meteorology Commons

Share Feedback About This Item

HALMOS COLLEGE OF NATURAL SCIENCES AND OCEANOGRAPHY

SPECIES SPECIFIC MICROCALCIFICATION IN REEF BUILDING CARIBBEAN CORALS IN OCEAN ACIDIFICATION CONDITIONS

By

Ashley M. Dungan

Submitted to the Faculty of
Halmos College of Natural Sciences and Oceanography
in partial fulfillment of the requirements for
the degree of Master of Science with a specialty in:

Marine Biology

Nova Southeastern University
November 13, 2015

ACKNOWLEDGEMENTS

TABLE OF CONTENTS

LIST OF TABLES

LIST OF FIGURES

Abstract

Coral reefs are one of the most economically important ecosystems on the planet, supplying roughly $30 billion USD annually into world economies from the goods and services they provide. Despite their great contribution to the world economy, anthropogenic influence via carbon dioxide emissions is leading to unprecedented changes in the tropical oceans with concerns about subsequent negative impacts on reefs. Surface ocean pH has dropped 0.1 units in the past century, representing a thirty percent increase in hydrogen ion concentration. In spite of this rapid shift in oceanic chemistry, it is unclear if individual species of Caribbean stony corals will be more affected or if there are differences in the responses at separate life stages for the impact of ocean acidification on calcification. Examined is the relationship between CO_2-induced seawater acidification, net calcification, photosynthesis, and respiration in three model Caribbean coral species: *Orbicella faveolata*, *Montastraea cavernosa*, and *Dichocoenia stokesi*, under near ambient (465 ± 5.52 ppm), and high (1451 ± 6.51 ppm) CO_2 conditions. Corals were exposed to each treatment for twelve to fifteen weeks and sampled at regular intervals. At each time point, a series of physiological responses were assessed: net and instantaneous calcification, gross photosynthetic rate, respiration rate, and tissue and skeletal differences utilizing electron microscopy. A species specific response was observed for net calcification; *D. stokesi* and *M. cavernosa* displayed a significant reduction in $CaCO_3$ secreted under OA conditions, while *O. faveolata* fragments showed no significant difference. At the cellular level, transmission electron micrographs verified that all species and treatments were actively calcifying. Skeletal crystals nucleated by *O. faveolata* in the high CO_2 treatments were statistically longer relative to controls indicating that skeleton formation was different in this treatment.

These results suggest that the addition of CO_2 may cause a shift in the overall energy budgets causing a modification of skeletal aragonite crystal structures, rather than inhibiting skeletal crystal formation. Consequential to this energy shift, *Orbicella faveolata* belongs in the category of Scleractinian corals that exhibit a lower sensitivity to ocean acidification, and existing colonies may continue to calcify and build reefs in the face of ocean acidification. It remains unclear, however, what the long term effects of a more acidic ocean may be on gamete production, immune response, and lesion recovery rates.

Key words: *Orbicella faveolata*, *Dichocoenia stokesi*, *Montastraea cavernosa*, electron microscopy, ultrastructure, climate change, calcification

<center>**Chapter 1**</center>

1 Introduction

1.1 Importance of Coral Reefs

Florida is home to the only living coral reef in the continental United States and the third longest barrier reef in the world (Chiappone and Sullivan 1996). Coral reefs are highly productive ecosystems that provide a variety of valuable goods and services to humans (UNEP 2006). These ecosystems are perhaps the most economically important on the planet while making up less than 0.2% of the sea floor (Cesar et al. 2003). The net present value of the world's coral reefs have been assessed at nearly $800 billion USD (Cesar et al. 2003). Coral reefs introduce approximately $30 billion USD annually into world economies from the goods and services they provide including recreation and tourism, commercial fisheries, and coastal protection (Costanza et al. 1997; Cesar et al. 2003; Brander and van Beukering 2013). Despite the provision of multiple services, factors such as pollution, overfishing, invasive species, excessive predation, disease, and global climate change, have led to the decline of coral reefs (Pandolfi et al. 2011). Nearly one fifth of the world's coral reefs have gone extinct and another 30% of coral reefs are expected to be lost in the coming decades unless the factors listed above, particularly the effects of global climate change, are mediated (Vernon et al. 2009).

Coral reefs are among the most diverse ecosystems on the planet; over 600,000 species have been documented worldwide (Knowlton 2001). As diversity is directly related to habitat size, decreasing living reef coverage as a result of anthropogenic influence will lead to future species extinctions (Cury et al. 2003). The coral species at the greatest risk are those that are long-lived and rarely recruited to new reefs, but serve as the structural foundation for the entire coral reef ecosystem. The animals in this group

are represented by hermatypic scleractinian corals. Coral population densities and overall health is a limiting factor for the survival of higher trophic organisms as they are the major source of nutrients and shelter in oligotrophic near shore waters (Cury et al. 2003). Coral reefs create a nutrient oasis in highly oligotrophic tropical waters in which dissolved inorganic carbons are converted to energy via photosynthesis. In corals this energy is passed directly from the *Symbiodinium sp.* producers to the animal host where it is used, among other things, to metabolize organic compounds resulting in nutrient rich waste products. Communities of marine plants and algae, fish, and invertebrates rely on this nutrient source as a means of survival. This process, in which corals support a range of higher trophic level species, is referred to as bottom-up control and allows coral to indirectly influence higher level organisms. In addition to supporting their own diverse set of organisms, coral reefs also protect and are reliant on sea grass beds and mangroves – both ecosystems are rich in biodiversity and serve as nursery systems for juvenile coral reef fish (Gattuso and Hansson 2011).

1.2   Ocean Acidification

Rapidly rising anthropogenic addition of carbon dioxide into the atmosphere is changing the chemical composition of seawater at a measurable and alarming rate. For decades global warming and climate change have dominated the scientific agenda. The so called "other CO_2 problem," ocean acidification (Brewer and Barry 2008; Doney et al. 2009), however, has recently become a popular topic in marine research. Over the past decade marine scientists have been examining the effects of ocean acidification on the biological, chemical, and physical components of the ocean (Kleypas et al. 2006; Sponberg 2007; Brewer 2009; Vernon et al. 2009; Ries et al. 2010; de Putron et al. 2011; Comeau et al. 2012). Carbon dioxide emissions, driven by human contamination

exceeding natural levels, are expected to result in a 2-4°C surface ocean temperature rise and a 0.4 pH unit decrease by the end of the century (Calderia and Wicket 2003; Raven et al. 2005; IPCC 2013). These changes in pH are developing 100 times faster than any records of the past hundreds of millennia (Calderia and Wicket 2003; Raven et al. 2005). Yet, little is known about how long term seawater acidification, increased carbon dioxide partial pressure, and the pH associated changes to ocean chemistry will influence marine organisms (Turley et al. 2006).

United States carbon emissions have risen drastically since the Industrial Revolution. Anthropogenic derived carbon released into the atmosphere will reach one of three fates: remain in the atmosphere, be absorbed into the terrestrial biosphere, or be taken up into the ocean (Raven et al. 2005). Carbon dioxide moves freely from the atmosphere into the water column as it diffuses down the concentration gradient to reach equilibrium. The ocean absorbs 10^6 metric tons of CO_2 per hour (Brewer 2009), corresponding to a quarter of the global carbon dioxide emitted from the burning of fossil fuels, deforestation, and cement production (Le Quere et al. 2009), thus reducing the effects of global warming, but creating the crisis of ocean acidification. This rapid exchange of carbon dioxide between the surface ocean waters and the atmosphere has led to a drop in ocean pH by 0.1 units (Sponberg 2007). As pH is on a log scale, this seemingly small drop represents a 30% increase in the number of hydronium ions present in surface seawater.

In May 2013, the atmospheric concentration of carbon dioxide measured at Mauna Loa Observatory, Hawaii, reached 400 ppm (see www.CO2Now.org). For the first time in the history of humankind, on average for every one million molecules in the

atmosphere, 400 of them were CO_2. Approximately 50% of this increase has occurred in the last three decades (Feely et al. 2009). In fact, for the past ten years the average annual rate of increase has been 2.07 parts per million (ppm), more than double the rate of increase in the 1960s (0.9 ppm year^{-1}) (Arenasa et al. 2014). In the past 420 kyr, atmospheric carbon dioxide rates have not exceeded 300 ppm (Petit et al. 1999). Our current atmospheric condition is unprecedented (Petit et al. 1999; Raven et al. 2005; Hoegh-Guldberg et al. 2007).

In seawater, gaseous carbon dioxide reacts to form carbonic acid (Kleypas et al. 1999a). Carbonic acid (H_2CO_3) is a weak acid and separates into its constituents based on pH. Under standard ocean conditions (pH 8.2-8.0) bicarbonate (HCO_3^-) concentration averages 6-10 times higher than that of carbonate (CO_3^{2-}). However, as CO_2 dissolves, more H^+ ions are released, decreasing the pH, and driving the reaction toward
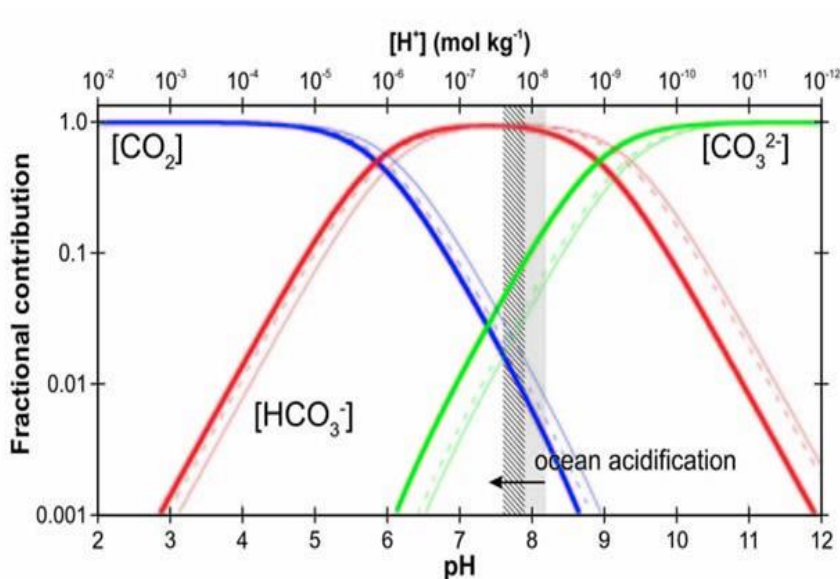
Figure 1.1: Bjerrum plot showing the range of relative proportions of [HCO_3^-], [CO_3^{2-}] and [CO_2] to DIC in seawater taking different temperature, salinity and pressure zones into account. The shaded region reflects the range of current ocean surface, while the hashed region reflects the corresponding projected year 2100 range: taken from the global ocean geochemistry model projections of Turley et al. (2010).

bicarbonate (Kleypas et al. 1999a) (Fig. 1.1). Following Le Chatelier's principle, the balanced reaction shows that as carbon dioxide increases, the reaction is driven toward the products, making carbonate less bioavailable (Eq. 1.1). The decline in pH since the Industrial Revolution has led to a reduction of carbonate ion concentrations by nearly 200 μmol kg^{-1} seawater (Hoegh-Guldberg et al. 2007).

Evidence from the end-Permian mass extinction provides insight into the potential future that we are creating via uncontrolled carbon dioxide emission rates. Characterized by high atmospheric levels of CO_2 through the eruption of the Siberian trap basalts, which expelled $10^{17} - 10^{19}$ mol CO_2, the end-Permian, mass extinction led to the extermination of over 85% of marine animals that formed a calcium carbonate skeleton proportionally larger than the supporting organic tissue (Knoll et al. 2007). The mechanism of this death has been attributed to multiple factors including hypercapnia, a condition characterized by elevated levels of carbon dioxide in blood, thus reducing the capacity of respiratory components to oxygenate tissues, oxygen depletion, and global warming (Knoll et al. 2007). Current concerns regarding the health of marine calcifiers mimic these causes, though particularly disturbing is the present rapid, unbuffered increase in pCO$_2$.

1.3   Future Scenarios

For the past thirty years the rate of carbon dioxide emissions into the atmosphere has been 1.79 ppm year^{-1} (IPCC 2013). This rate may be the deciding factor in the future of marine calcifiers, as it is two to three orders of magnitude higher than rates recorded for the past 420,000 years (Hoegh-Guldberg et al. 2007; Knoll et al. 2007). The International Panel on Climate Change (IPCC) created a family of scenarios to predict future emission rates which provides the scientific community a standard set of values for

experimentation. The Special Report on Emissions Scenarios (SRES) outlines four simulations of our 2100 atmosphere; scientists have used these scenarios to predict what

Table 1.1: The four representative concentration pathways (RCP) developed under the IPCC AR4. Presented by Moss et al. (2010).

Name	Radiative forcing	Concentration(p.p.m.)	Pathway
RCP8.5	>8.5 Wm^{-2} in 2100	>1,370 CO_2-equiv. in 2100	Rising
RCP6.0	~6 Wm^{-2} at stabilization after 2100	~850 CO_2-equiv. (at stabilization after 2100)	Stabilization without overshoot
RCP4.5	~4.5 Wm^{-2} at stabilization after 2100	~650 CO_2-equiv. (at stabilization after 2100)	Stabilization without overshoot
RCP2.6	Peak at ~3 Wm^{-2} before 2100 and then declines	Peak at ~490 CO_2-equiv. before 2100 and then declines	Peak and decline

the atmospheric carbon dioxide concentrations may be in the future (Table 1.1).

Changes in the atmosphere, land, ocean, biosphere, or cryosphere both natural and anthropogenic, can perturb the Earth's radiation budget, producing a radiative forcing (RF) that affects climate. The Earth's surface temperature is determined by the energy balance between incoming solar radiation and outgoing infrared radiation. Radiative forcing is the measurement of the capacity of a gas or other forcing agents to influence that energy balance, thereby contributing to climate change (IPCC 2013). Global warming occurs when there is an increase in Earth's energy budget causing a positive radiative forcing. Because Greenhouse Gases (GHG's) absorb infrared radiation and re-emit it back to the Earth's surface, thus increasing the Earth's energy balance, they have positive RF values. The radiative forcing of a GHG, such as carbon dioxide, is determined by its atmospheric concentration, warming capacity, residence time, and spatial distribution (IPCC 2013).

Four representative concentration pathways (RCP's) were developed to map possible outcomes for the composition of the atmosphere (Fig. 1.2). These RCPs were designed to capture four possible futures: two in which there is little to no coordinated action on reducing global emissions (worst case – RCP8.5 and best case – RCP6.0) and two where there is serious global action on climate change (worst case – RCP4.5 and best case – RCP 2.6). Simply, RCP8.5 represents 'business as usual,' where there is strong economic development for the rest of this century, driven primarily by dependence on fossil fuels (IPCC 2013). RCP6.0 represents a world that has not developed a global coordinated climate policy, but where many localized clean energy initiatives manage to stabilize emissions by the latter half of the century. RCP4.5 represents a world that implements strong limits on fossil fuel emissions, leading to a peak in GHG emissions by mid-century that then start to fall. RCP2.6 represents a world where emissions peak in the next few years, and then fall considerably, so that the world becomes carbon neutral by about mid-century.

The current level of radiative forcing, according to the IPCC AR4, is 1.6 Wm^{-2} (IPCC 2013). Considering the terrestrial surface area of the Earth, this results in a current total warming of about 800 terawatts — more than 50 times the world's average rate of energy consumption, which is currently about 15 terawatts. However, in projections that model our current trend, RCP8.5, RF levels reach 8.3 Wm^{-2} in 2100 on a rising trajectory. This project exposed corals to pCO$_2$ levels forecast by the RCP8.5 scenario: present day (~400 ppm) and year 2100 (>1370 ppm).
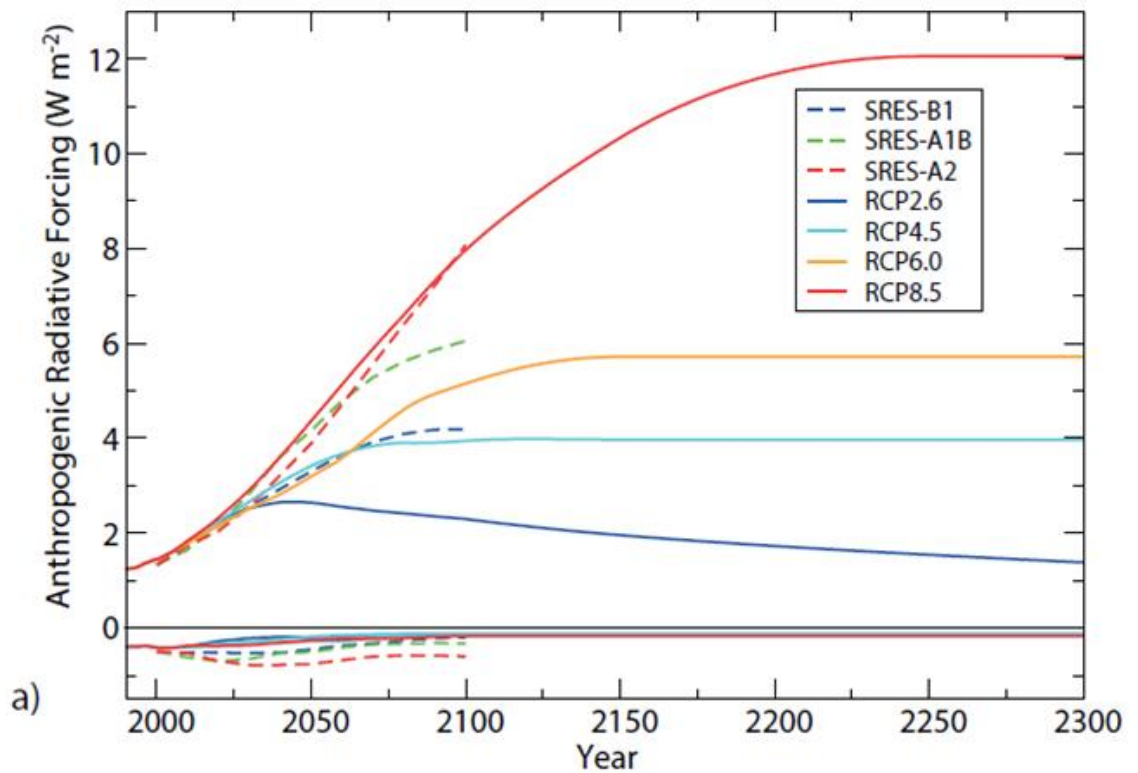
Figure 1.2: Time evolution of the total anthropogenic radiative forcing (RF) relative to pre-industrial (about 1765) between 2000 and 2300 for RCP scenarios as computed by the Integrated Assessment Models (IAMs) used to develop those scenarios. Taken from the IPCC's Fifth Assessment Report, Working Group 1, Chapter 12, Figure 12.3a (IPCC 2013).

1.4   Skeleton Formation

Calcium carbonate marine skeleton is deposited as high magnesium calcite (echinoderms), aragonite (corals and mollusks), or calcite (coccolithophores and foraminifera) (Raven et al. 2005). Each arrangement of the molecular structure results in a different solubility; high magnesium calcite is the most soluble followed by aragonite, then calcite (Andersson et al. 2008). Caribbean scleractinian corals almost exclusively deposit aragonite skeletons. The process of calcification is controlled by the concentration of calcium and carbonate in the calcifying matrix. The saturation state of aragonite (Ω_{arag}) is a measure of super-saturation of this mineral phase in seawater and is measured as $\dfrac{[Ca^{2+}]unk\,[CO_3^{-2}]unk}{[Ca^{2+}][CO_3^{-2}]}$ (Equation 2), where the values in the denominator correspond

to 100% saturation (Kleypas et al. 1999a; Kleypas et al. 1999b; Raven et al. 2005). Calcium displays conservative properties in seawater, thus, saturation state is based predominately on carbonate availability (Cohen and Holcomb 2009). At lower pH values, carbonate is less biologically available, therefore lowering the saturation point of all mineral forms of calcium carbonate. One hundred years ago, Ω_{arag} averaged 4.6 ± 0.2 (± 1 SD) in tropical regions. Today, these regions average 4.01 ± 0.17 (Gledhill et al. 2008). This value is predicted to decrease 0.8 by 2065 and another 0.3 by 2100, potentially resulting in an aragonite saturation of 2.8. Trends in global aragonite saturation have shown a transition from coral reef to algal communities near Ω_{arag} values of 3.4 (Kleypas et al. 1999a). Theoretically, when Ω_{arag} is greater than 1, aragonite should precipitate and if Ω_{arag} is less than 1, aragonite will dissolve (Kleypas et al. 1999a). However, there are kinetic barriers that require higher saturation states for calcification to occur (Cohen and Holcomb 2009). To make calcification more favorable, corals grow their crystals in a semi-isolated compartment that allows them to modify and control the carbonate chemistry of the calcifying fluid. Newly formed skeleton is surrounded by four layers of coral tissue, forming a barrier around the skeleton to avoid direct contact with seawater (Fig. 1.3, Cohen and Holcomb 2009).

Aragonite is produced as micron sized crystals that nucleate, grow, and are packed into intricate bundles to form new skeleton (Al-Horani et al. 2003). Corals are actively calcifying at all times; the calicoderm, a layer of epithelia on the aboral surface of each polyp comprised of simple squamous cells (Glynn et al. 1985), functions to facilitate ion transport to create favorable conditions for skeletal secretion. Coral calcification occurs in the extracellular space beneath the coral polyp calicoderm. In order for calcification to occur, corals must surpass a kinetic threshold based on

bicarbonate to carbonate ratios. Ca-ATPase is used to transport Ca^{2+} to the skeletal deposition site in exchange for H^+. This ion exchange leads to concentration increases in both calcium and carbonate in the subcalicoblastic space (Fig. 1.3, Al-Horani et al. 2003). By pumping hydronium ions out of this space, thus increasing the pH, bicarbonate is converted to the skeleton forming carbonate ion. The pH of the calicoblastic fluid has been measured at 9.3 during the day, corresponding to an aragonite saturation state of 25 even though external seawater measured 8.1 and 4, respectively (Al-Horani et al. 2003). Removal of hydronium ions to reach a suitable concentration of carbonate is required to facilitate skeletal production (Equations 3 and 4).

Equation 3: $Ca^{2+} + CO_2 + H_2O \rightarrow CaCO_3 + 2H^+$

Equation 4: $Ca^{2+} + HCO_3^- \rightarrow CaCO_3 + H^+$
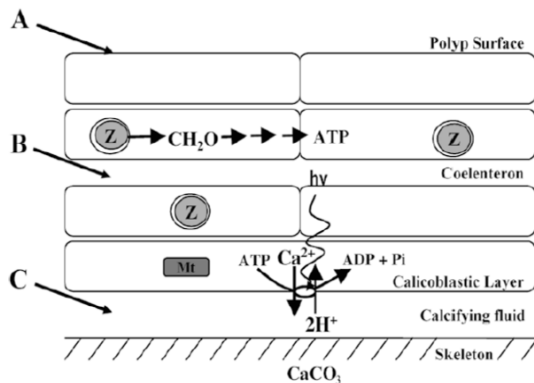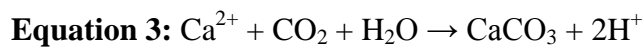
Figure 1.3: A conceptual model of light-enhanced coral calcification taken from Al-Horani et al. (2003) where A-C represents the surface of the epidermis, the gastrodermis, and the sub-calicoblastic space respectively.

The space below the calicoderm contains a fluid originating from seawater. As seawater becomes less basic through ocean acidification, carbonate concentration decreases and more energy will be required to remove H^+ to the point where calcification is thermodynamically favored (Al-Horani et al. 2003). When pH levels drop, more carbonate ions are converted into bicarbonate ions. Although bicarbonate is a component of the calcification reaction (Equation 4), the percent increase in bicarbonate from acidified conditions will not be significant enough to compensate for the reduction of

carbonate (Comeau et al. 2012). Once the oceanic carbonate source is exhausted, carbonate ions will be removed from previously calcified substances, such as coral skeleton. If the ocean reaches a pH low enough to cause undersaturation of aragonite in the calicoblastic fluid, coral skeleton dissolution will be thermodynamically favored.

1.5   Background Studies

The mechanism of biological coral calcification is not fully understood (Cohen and McConnaughey 2003; Cohen and Holcomb 2009; Allemand et al. 2011; Ries 2011; Comeau et al. 2012). This is in part due to the location of the subcalicoblastic space. Therefore, abiogenic aragonite accretion under laboratory conditions has been used to compare the composition and morphology of newly formed coral aragonite skeleton formed under various aragonite saturation states (Cohen and Holcomb 2009). Abiogenic aragonite crystals grew, displaying a morphological resemblance to those grown biologically by coral. Nucleation occurred at $\Omega_{arag} > 20$ (high saturation), while growth of these crystals was favored at $\Omega_{arag}= 6$-19. Crystal morphology changed gradually through reduced saturation states from long, thick, blade-like crystals at $\Omega_{arag}=20$ to short, wide, highly faceted crystals at $\Omega_{arag}=6$. The results of this study have important implications for studies of coral growth under various aragonite saturation states, nevertheless skeletal structures for most Caribbean species have not been documented under ambient or high CO_2 conditions.

Primary polyps (new recruits) of the Atlantic golf ball coral *Favia fragum* secrete aragonite under simulated ocean acidification conditions creating an aragonite saturation state (Ω_{arag}) of $\Omega_{arag}=0.22$ (Cohen et al. 2009). Saturation states less than one should theoretically lead to dissolution (Kleypas et al. 2006; Cohen and Holcomb 2009) These corals were able to create an internal environment elevating the carbonate concentrations,

through acid base regulation mechanisms. However, skeleton formation in low aragonite saturation lagged days behind calcification in ambient conditions. Aragonite crystals have been quantified undergoing gradual changes in the size, shape, orientation, and composition based on aragonite saturation state (Cohen et al. 2009; Fig. 1.4). Crystal morphology changes from a blade-like crystal that has a high length to width ratio to crystals that are flatter and rhombic in shape as seawater pH and therefore Ω_{arag} drop. Interestingly, the shape of the coral basal plate became irregular as saturation state decreased. These basal plate anomalies, in conjunction with an incomplete rim, can prevent an effective seal around the calcifying region. External seawater in the calcifying fluid will exacerbate the challenges for calcification the organism is already experiencing in a low pH environment. Successful calcification is dependent on an organism's ability to achieve supersaturation in their calcifying fluid. Future success of marine calcifying organisms in a high CO_2 environment could be based on an individual's ability

Figure 1.4: Scanning electron micrographs showing progressive changes in Favia fragum corallite development including reduced growth of septa and shrinking of the basal plate (A-D). E-H show the changes in crystal morphology that occur as saturation state decreases. Saturation states being compared are Ω_{arag}=3.71 (A, E), Ω_{arag}=2.40 (B, F), Ω_{arag}=1.03 (C, G) and Ω_{arag}=0.22 (D, H). Taken from Cohen et al. 2009.

12

to overcome this limitation (Cohen et al. 2009).

The significance of bicarbonate and carbonate concentration in seawater for *Favia fragum* and *Porites astreoides* new recruit initial calcification has been examined (*d*e Putron et al. 2011). In this study carbonate chemistry parameters were used to determine the saturation state of the experimental seawater. Larvae were allowed to settle on tiles and exposed to treatment CO_2 conditions (394 ± 9, 753 ± 12, and 2327 ± 23 ppm) for two weeks. After the experimental period, polyps were bleached to remove coral tissue and the corallite skeleton was weighed on a microbalance. The results showed a negative correlation between the skeletal growth of new recruits and Ω_{arag} for both species. This data, paired with that from Cohen et al. (2009), shows that while new *F. fragum* recruits are able to calcify under low aragonite saturation states, there is a change in the morphology of new skeletal crystals and mass is negatively impacted. It has not been established however, how calcification for adults and new recruits of the same species respond to low pH conditions.

This work is a comparative study of the effects of high CO_2 on calcification in three adult coral species including newly settled spat from the threatened *Orbicella faveolata* commonly found in the Florida Reef Tract . Since survivorship at every life stage is necessary for organismal survival and development of future generations, analyzing life stage response differences may reveal the developmental stage most vulnerable to ocean acidification. As suggested by Findlay et al. (2009), organisms may be able to adapt by up-regulating calcification or change mineral production in response to increased acidity of seawater. This project seeks to evaluate this concept as well as determine the impact of high CO_2 on coral calcification by raising coral adults

(*Dichocoenia stokesi*, *Montastraea cavernosa*, and *O. faveolata*) and new recruits (*O. faveolata*) in two high CO_2 environments based on the RCP8.5 IPCC scenario.

1.6   Objectives

Ocean associated changes in pH are occurring 100 times faster than in the indicated by past records of hundreds of millennia (Petit et al. 1999; Caldeira and Wickett 2003; Raven et al. 2005); yet, little is known about how long-term seawater acidification, increased carbon dioxide partial pressure, and the pH associated changes to ocean chemistry will influence the calcification of hermatypic corals (Kleypas et al. 2006). Calcification utilizes up to 20% of a coral's energy budget (Cohen and McConnaughey 2003). Assuming constant availability of nutrients and food, the energy budget for many hard corals is fixed, and they can only allocate a fixed amount of energy for calcification. Under low pH conditions this may result in incomplete removal of excess protons and secretion of a weaker and poorly packed skeleton. The success of a coral reef is dependent upon the intricate relationships that exist between the coral's vertical structure and other organisms in the environment. Changes in coral calcification due to ocean acidification can negatively influence the quality and characteristics of the reef structure, potentially leading to shelter loss and food shortage for other organisms in the reef community. This research was conducted to address two specific and distinct questions:

1. **Will decreased pH affect fine scale calcification in *O. faveolata* recruits and adults?**

    To address this question, analyses will be conducted to assess differences in calcification between *O. faveolata* juveniles and adults, after being exposed to the experimental conditions for two weeks and three months, respectively. Successful recruitment and survival of a species is dependent on success at every

life stage; therefore, interruptions during either early polyp growth or adult calcification could hinder the success of a species. It has been observed that as pH decreases and pCO$_2$ increases, coral calcification and skeletal crystal development will become more rhombic in shape and less blade-like (Cohen and McConnaughey 2003; Cohen and Holcomb 2009; Cohen et al. 2009). In this study (?) crystal length measurements of scanning electron microscopy (SEM) micrographs are quantified in ImageJ (NIH).

2. **Are *M. cavernosa* and *D. stokesi* able to acclimate under persistent exposure to high pCO$_2$ conditions*?***

Corals were maintained in ambient and high CO$_2$ treatment water for fifteen weeks and sampled periodically for scanning and transmission electron microscopy. Additionally, fragments were weighed to evaluate growth as measured by the addition of new calcified material. The resulting data shows that in these corals calcification was not different, or that fifteen weeks was not a long enough for changes to occur.

Chapter 2

Systemic to microscale response of *Orbicella faveolata* to future ocean CO_2 conditions

2.1   Introduction

United States carbon emissions have risen drastically since the Industrial Revolution when the atmospheric concentration of carbon dioxide was approximately 280 parts per million (ppm). In May 2013, carbon dioxide concentrations, measured at the Mauna Loa Observatory in Hawaii, reached 400 ppm (see www.CO2Now.org). The rate of carbon dioxide emission into the atmosphere over the past thirty years has been 1.79 ppm year^{-1} (IPCC 2013); this time span has attributed to roughly 50% of the global change in carbon dioxide concentrations since the late 1700's (Feely et al. 2009). Our current condition is unprecedented over the past 800,000 years (Petit et al. 1999; Raven et al. 2005; Hoegh-Guldberg et al. 2007; Lüthi et al. 2008).

Over a quarter of all carbon dioxide released post Industrial Revolution has been absorbed by the oceans (Calderia and Wicket 2003; Sabine et al. 2004; Sponberg 2007). Although mitigating the effects of global warming, the 'oceanic sink' (Sabine et al. 2004) of carbon dioxide is expected to result in a 0.4 pH unit decrease in the surface oceans by the end of the century (Calderia and Wicket 2003; Raven et al. 2005; IPCC 2013). This associated change is progressing 100 times faster than any climate recording oceanic pH for the past hundreds of millennia (Calderia and Wicket 2003; Raven et al. 2005). Yet, little is known about how long term seawater acidification, increased carbon dioxide partial pressure, and the pH associated changes to ocean chemistry will influence marine organisms (Turley et al. 2006).

The seawater changes due to rapidly rising anthropogenic addition of carbon dioxide into the atmosphere predicted for the end of the century present major challenges

for calcifying organisms. Coral reefs are among the most diverse ecosystems on the planet; over 600,000 species have been documented worldwide (Knowlton 2001). The vast diversity is due to the structurally complex calcium carbonate foundation of coral reef ecosystems. Yet, this rugosity is at risk for degradation by ocean acidification (Fabricius et al. 2011; Silbiger and Donahue 2015). The species at the greatest risk are hermatypic scleractinian corals that are long-lived and rarely recruited to reefs, but serve as the structural foundation for the entire coral reef ecosystem. Nearly one fifth of the world's coral reefs have gone extinct and another 30% of coral reefs are expected to be lost in the coming decades unless the effects of global climate change are mediated (Vernon et al. 2009; Pandolfi et al. 2011).

Biogenic calcification occurs within a physiologically controlled environment (Al-Horani et al. 2003; Cohen and McConnaughey 2003; McCulloch et al. 2012; Holcomb et al. 2014), with scleractinian coral precipitating their calcium carbonate skeleton from an extracellular calcifying fluid in a semi-isolated space (Al-Horani et al 2003; Venn et al. 2011). Corals are able to raise the pH of this fluid during active calcification in order to promote the dissolved organic carbon (DIC) components to shift toward carbonate (Al-Horani et al. 2003; Holcomb et al. 2014); this is an energy expensive process. Net calcification has typically been shown to decline after exposure to climate stressors such as ocean acidification, likely in part to the altered energy budget (Langdon and Atkinson 2005; Schneider and Erez 2006). The magnitude of the decline differs across species and is highly variable (Anthony et al. 2008; Ries et al. 2009, de Putron et al. 2011; Pandolfi et al. 2011; Silbiger and Donahue 2015). Recent work has found that, although net calcification is declining, corals are still secreting new skeletal material (Cohen et al. 2009; McCulloch et al. 2012; Enochs et al. 2014; Holcomb et al.

2014; Tambutté et al. 2015). Successful calcification is dependent on an organism's ability to achieve supersaturation in their calcifying fluid; this process is limited by energy requirements (McCulloch et al. 2012). Future success of marine calcifying organisms in a high CO_2 environment could be based on an individual's ability to overcome this limitation (Cohen et al. 2009).

To date, there have been several studies that evaluated the responses of adult corals (Anthony et al. 2008; Marubini et al. 2008; Holcomb et al. 2012; Moya et al. 2012; Schoefp et al. 2013; Enochs et al. 2014; Holcomb et al. 2014; Tambutté et al. 2015), juveniles (de Putron et al. 2011; Drenkard et al. 2013) or larval physiology and settlement (Albright et al. 2008; Cohen et al. 2009; Albright et al. 2010; Albright and Langdon 2011; Cumbo et al. 2013) under ocean acidification conditions. However, there still remains a gap in knowledge as many projects have included only a few species. This work is a comparative study of the effects of high CO_2 on the recently listed threatened species, *Orbicella faveolata*, which is a common reef building species, by rearing adult and new recruits in either seawater simulating the present environment or a high CO_2 environment based on the representative concentration pathway 8.5 (RCP8.5) IPCC scenario predicted for year 2100. RCP8.5 represents 'business as usual,' where there is strong economic development for the rest of this century, driven primarily by dependence on fossil fuels (IPCC 2013).

I present the results of an experimental study designed to examine the effect of lowered ocean pH, reduced carbonate concentrations, and high $p$$CO_2$ on the microcalcification in *Orbicella faveolata*. Several physiological parameters were evaluated in order to address the question, "Will decreased pH affect fine scale calcification in *O. faveolata* recruits and adults?" I examined the impact of increased

pCO$_2$ on net calcification on *O. faveolata* adults through buoyant weights and alkalinity anomaly. Productivity, which is expected to be influenced by an altered carbonate chemistry (Anthony et al. 2008), was documented as oxygen production and consumption via photosynthesis and respiration. Using scanning electron microscopy of both adults and new recruits, I was able to compare the crystal structure of newly deposited calcium carbonate across treatment conditions.

2.2   Methods

2.2.1   *Coral collection*

To represent the crucial framework builders on Caribbean coral reefs, I chose the recently IUCN listed threatened species, *Orbicella faveolata*. Considered one of the primary reef-building corals in the Caribbean, *Orbicella faveolata* is one of the top-ten most abundant scleractinian corals (Miller et al. 2013). Formerly known as *Montastraea faveolata* (Ellis and Solander 1786), the genus changed in 2012 following a molecular and morphometric analysis (Budd et al. 2012).

Orbicella faveolata adults were collected on June 23rd on a patch reef off Mote's Tropical Research Laboratory (TRL) in Summerland Key, FL. Colonies were transported to Mote Marine Laboratory (MML), Sarasota, FL, in seawater saturated bubble wrap, where they were fragmented into large sections and allowed to acclimate in the flow through system (OASys) for two days. After nine weeks of exposure fragments were harvested from the remaining large pieces using a 7" wet tile to remove tissue that may have been contaminated with black band disease. Fragments were approximately 4-9 cm^2. I acknowledge that this approach may have affected the response for adult *O. faveolata* in this experimental setup and care was taken to collect data that accurately reflect how low pH environments in the absence of disease influence calcification. Each tank was supplied with filtered seawater (30 μm) and exposed to T5 fluorescent actinic and daylight bulbs, providing an average of 80 μmol m^{-2} s^{-1}. Lights were set to a 12h light/dark cycle. Corals were fed three times per week ad libitum with a blend of marine microalgae (Phyto-Feast).

Orbicella faveolata spat were settled from spawning events and pooled from 2 cohorts: one spawned August 16th, 2014 (from Horseshoe reef, Key Largo, FL; ~ 2

genets) and the other August 17th (combined from Horseshoe and Grecian Rocks reefs; ~ 8 genets total) (M. Miller and X. Serrano pers. comm.). Larvae were settled onto ceramic plugs at a field station in Key Largo, FL. The plugs had been conditioned off-shore at Sand Island Reef off Key Largo for three weeks prior to settlement. Forty plugs with *O. faveolata* spat were transported to MML in Sarasota, FL on September 6th where twenty-seven plugs with identified spat were distributed to eight experimental tanks containing *Montastraea cavernosa* and *Dichocoenia stokesi* fragments (see Chap. 3). *Orbicella faveolata* spat were reared in ambient and low pH seawater for two weeks, approximately three weeks after settlement when initial calcification begins (M. Miller and X. Serrano, pers. comm.).

2.2.2   Experimental Design

Ambient seawater was pumped into the system from Sarasota Bay, where it was treated by ozonation and sand bed filtration to remove particles in excess of 30 μm. A 65 gallon degas tank tempered the pH of incoming seawater through aeration from an outdoor air pump connected to two large air stones sitting at the bottom of the tank. In the degas tank water temperature was maintained at 25°C (Delta Star in-line water chiller, Aqua Logic, Inc., Hydortheo submersible, 50-100 watt heaters). Water was transferred from the degassing tank through a bulkhead at the bottom to an external pump to each of the treatment header tanks. Both ambient and high CO_2 tanks contained a pH probe, temperature probe, and circulation pump. The high CO_2 tank also contained a CO_2 gas line, which ran to a CO_2 tank and electronic regulator to manipulate pCO_2. Levels of acidification were regulated through a pH stat system (Apex Neptune Jr. Controller with pH probe module) set to pH target values of 8.10 and 7.70, corresponding to CO_2 concentrations of 450 ppm and 1450 ppm for the ambient and high CO_2 dosing regimens,

respectively (Table 2.1). When the pH of this tank rises above a 7.7 point programmed into the apex controller (Neptune Systems), power to the electronic regulator is turned on and pure CO_2 is allowed into the acidified tank. Water flows through a bulkhead at the bottom of each of the header tanks and into a 1 inch supply manifold. Flow into each individual aquarium (four recruit tanks and one adult coral tank for each treatment) was sustained at 75 mL/min to allow for a complete turnover rate of approximately four hours. Each aquaria (19 liters) under is held in a water bath under a 12:12 hour light/dark regime (T5 Fluorescent Actinic pink and blue daylights).

pH was measured on the NBS scale using Lab Grade Neptune Systems pH probes, each connected to the logger/controller unit via a Neptune Systems Apex controller. The experimental CO_2 environments were chosen to represent the current atmospheric CO_2 levels and the RCP8.5 scenario presented in the International Panel on Climate Change (IPCC) Fifth Assessment Report (AR5), with year 2100 pCO$_2$ (ppm) >1370 ppm (IPCC, 2013; Moss et al. 2010) (Table 1). Daily measurements of pH (Mettler Toledo SevenGo pro), temperature (EcoSense EC300A), and salinity (EcoSense EC300A) were compiled with weekly total alkalinity (TA) to determine the distribution of carbon species and aragonite saturation state for all treatments (Table 2.1) using the program CO2SYS (Lewis and Wallace 1998). Sample collection and storage for TA was done in 120 mL borosilicate bottles that were cleaned with 10% HCl and rinsed three times with nanopure water. TA was measured using a modification of the open-cell titration method (Dickson et al. 2007, SOP 3b) on a Metrohm 916 Ti-Touch automated titrator using 0.05M HCl in 0.6M NaCl for 32 g seawater samples. All TA data was verified for accuracy using certified reference material (CRM) seawater from the Dickson Lab at Scripps Institute (Batch 137); samples were averaged +2.19% from the actual

value with a SE of 6.90 µmol kg^{-1}. CO2SYS was run using the K1K2 apparent equilibrium constants from Mehrback (1973) and refit by Dickson and Millero (1987), HSO$_4^-$ dissociation constants were taken from Uppstrom (1974) and Dickson (1990), and pH was on the NBS scale.

Table 2.1: Means (± standard errors) of all measured parameters by treatment header tank, representative of each aquarium. pCO$_2$, HCO$_3^-$, CO$_3^{2-}$, CO$_2$, DIC, and Ωarag were all calculated from measured TA and pH samples in CO2SYS.

Header Tank	Temperature (°C)	Salinity (psu)	pH (NBS)	Alkalinity (µmol kg^{-1})	pCO$_2$ (ppm)	DIC (µmol kg^{-1})	[CO$_2$] (µmol kg^{-1})	[HCO$_3^-$] (µmol kg^{-1})	[CO$_3^{2-}$] (µmol kg^{-1})	Ωarag
Ambient	25.77±0.07	34.96±0.04	8.14 ± 0.002	2441 ± 5.38	465 ±5.52	2126±8.48	12.4±0.21	1889±10.4	224.5±2.75	3.6 ± 0.05
High CO$_2$	26.35±0.06	34.98±0.05	7.65 ± 0.003	2443 ± 5.35	1451 ± 6.51	2333±5.71	38.1±0.27	2195±5.68	99.2±0.81	1.6 ± 0.01

2.2.3 Buoyant weight

Adult coral fragments were weighed as described by Davies (1989), using an Ohaus Adventure Pro analytical balance. During the weighing periods, corals were suspended on a platform approximately 15 cm into an aquarium filled with treatment seawater. Temperature and salinity were recorded after each mass and used to calculate seawater density; this remained constant at 1.023 mg/L. Calcification rate was quantified from the difference in buoyant wet weights between weeks 10 and 12 as *O. faveolata* adults were fragmented during week 9. Calcification was normalized to tissue surface area and expressed as mg CaCO$_3$ cm^{-2} d^{-1}.

2.2.4 Physiology

Because corals are a holobiont and calcification may be influenced by the activity of the mutualistic zooxanthellae and other organisms that make up the coral holobiont, productivity data was collected. Photosynthesis was measured as the oxygen production from each fragment for one hour under controlled artificial lighting (T9 fluorescent and 4

LED strip lights) matching the daytime OASys irradiances of 80 µmol m^{-2} s^{-1} and respiration measurements as oxygen consumption during a one hour period in complete darkness. Temperature was maintained at 25 °C using a recirculating water bath (PolyScience MX Circulating Water Bath). Calibrations were completed prior to each measurement using air saturated seawater and blank chambers were used to remove any metabolic signal from the water column. Photosynthesis and respiration measurements were conducted using four sealed, recirculating respirometry chambers with flow regimes simulating natural conditions, each chamber connected to a high-precision fiber-optic oxygen meter and logging system (FirestingO2, Pyro Science). Oxygen fluxes of all specimens were normalized to tissue surface area determined from geometric analyses of digital photographs (ImageJ, NIH).

2.2.5   Alkalinity Anomaly

For each light and dark hour in the respirometry chambers, a water sample was removed from the chamber and analyzed for total alkalinity using a modification of the open-cell titration method (Dickson et al. 2007, SOP 3b) on a Metrohm 916 Ti-Touch automated titrator using 0.05 M HCl in 0.6 M NaCl titrant for 32 g seawater samples. Water samples were filtered (0.2µm membrane filters) prior to analysis. This alkalinity anomaly method (Andersson et al. 2009; Silbiger and Donahue 2015) calculates net calcification from changes in total alkalinity from the equation $G = \left[\frac{dTA}{dt}\right]/2$, where $\left[\frac{dTA}{dt}\right]$ is the change in TA in the chamber during the measurement period (change in TA normalized to the volume of water and the surface area of the coral). This change in alkalinity over time is calculated from : $\frac{d\text{TA}}{dt} = \frac{TA_{aq,t2} - TA_{aq,t1}}{\Delta t * SA} * Vol * \rho$, where $TA_{aq,t1}$ = total alkalinity in the chamber at the first sampling time point (µEq kg^{-1}), $TA_{aq,t2}$ = total

alkalinity in the chamber at the second sampling time point (μEq kg^{-1}), Δt = time between first and second sampling time point (h), SA = surface area of the coral in the chamber calculated using ImageJ (cm^{-2}), Vol= volume of water in the chamber (L), and ρ = Density of seawater (kg L^{-1}). The final equation is divided by two because one mole of CaCO$_3$ is precipitated or dissolved for every two moles of TA removed or added to the water column. Here, G represents the sum of all the calcification processes minus the sum of all the dissolution processes in μmol CaCO$_3$ cm^{-2} h^{-1}; thus, all positive numbers are net calcification, and all negative numbers are negative net calcification (i.e., net dissolution). Net daytime calcification (Gday/ is calculated from the first sampling period in the light, net nighttime dissolution (Night/ is calculated from the second sampling period in the dark. Samples that could not be run immediately were stored in a 2°C refrigerator and processed within a week.

2.2.6   Electron Microscopy

At the end of twelve weeks a 2 cm^2 section of tissue and skeleton was removed from each of the adults using a dremel tool (Dremel 200). Juveniles were taken from the treatment conditions after one and two weeks. Samples were placed in a 50% NaClO solution in preparation for scanning electron microscopy (SEM). Juveniles were bleached while they were still attached to the plug to ensure no damage to the skeletons. After complete tissue removal, the fragments were rinsed with tap water, dried, and mounted on carbon adhesive-covered aluminum stubs and coated with palladium. Samples were imaged in an FEI XL-30 ESEM/SEM fitted with an Oxford EDS system at the University of Miami's Center for Advanced Microscopy. The columella region was targeted to image the crystal structure of newly calcified material. Images were analyzed in ImageJ

(NIH) to quantify the length of the largest crystals produced by each species and time period.

2.2.7   Statistical Analysis

The software program JMP was used to examine independent and interaction relationships between treatment variables. All response data to CO_2 treatments were tested using independent samples t-tests or one-way ANOVA's. Data were tested for variance homogeneity using Levene's test and normality using the Shapiro-Wilk test. Wilcoxon and Kruskal-Wallis tests were run for non-normal sample sets.

2.3   Results

2.3.1   Buoyant Weight

An independent-samples t-test compared *Orbicella faveolata* adult mean net calcification (mg $CaCO_3$ cm^{-2} d^{-1}) between the treatment conditions and no significant difference in *O. faveolata* growth rates between treatments was observed (n = 7 individuals, t-test, p>0.05).

2.3.2   Crystal Length

Settlement plugs were collected at random from each of the treatment tanks (n=4 per treatment) after one or two weeks and imaged using scanning electron microscopy (Fig. 2.1a). To evaluate differences in crystal length for *O. faveolata* adults and recruits between treatment conditions, independent subjects t-test were run. Where assumptions were not met, the Wilcoxon test was used. There was a significant increase in newly deposited crystals' length from ambient to high CO_2 seawater. This was the case for recruits after one (98%) and two (111%) weeks exposure, as well as for adults after twelve weeks (245%; Fig 2.1b, Table 2.2). These results indicate that there are similar responses to ocean acidification during the earliest calcification stages and mature adults.

Table 2.2: Results of t-test and descriptive statistics for crystal length by treatment for *Orbicella faveolata* recruits and adults.

	Ambient			High CO_2					
	M	SD	n	M	SD	n	t/Chi^2	df	p
*Week 1 recruits**	1.072	0.62	22	2.118	1.25	24	8.5542	1	0.0034
Week 2 recruits	0.653	0.64	19	1.381	0.49	15	3.625	32	0.0010
*Week 12 Adults**	0.647	0.32	15	2.232	0.87	20	22.090	1	< 0.0001

*Data run using Wilcoxon test
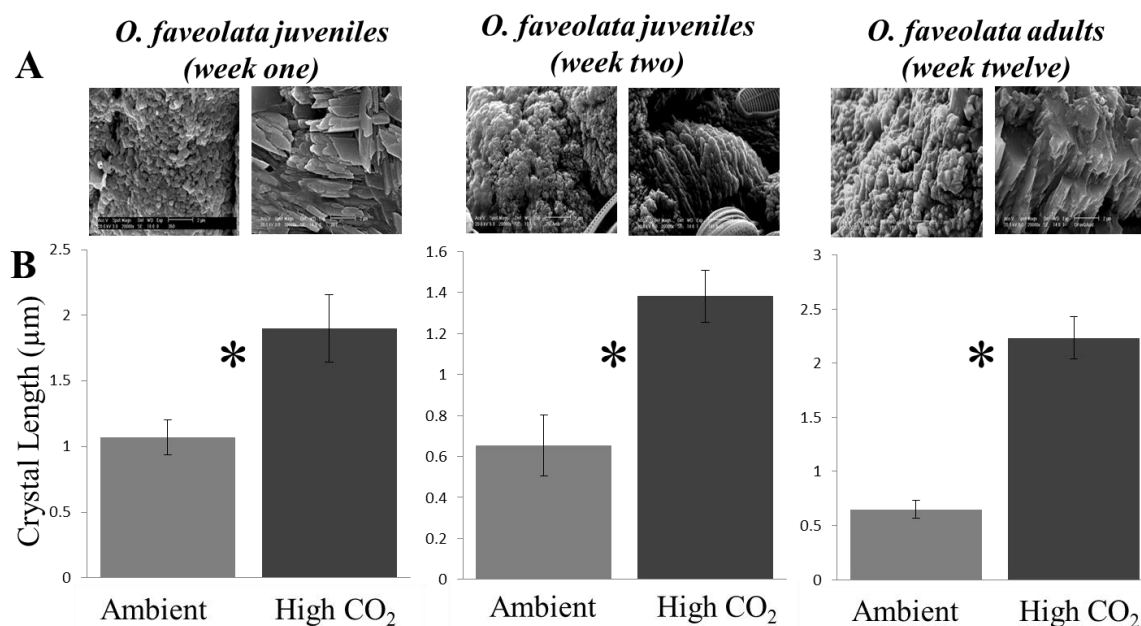
Figure 2.1: Average (mean ± SEM) crystal length (µm) determined from scanning electron micrographs for *O. faveolata* juveniles after one (n=4 per treatment) and two weeks (n=4 per treatment) of exposure and adults (n=7 per treatment) under ambient and high CO_2 conditions. Images are representative micrographs of the crystal structure in the respective treatment. Asterisks represent significant differences in treatment conditions determined using independent-samples t-test or the non-parametric Wilcoxon test where appropriate.

2.3.3 Physiology

Orbicella faveolata fragments' photosynthetic and respiration rates after twelve weeks in ambient and high CO_2 conditions were examined using an independent samples t-test. There was no significant differences in the effect of treatment on oxygen production or consumption through photosynthesis and respiration for this species during the final sampling period (n=7, t-test, p>0.05).

2.3.4 Alkalinity Anomaly

Orbicella faveolata fragments' mean light and dark calcification rates (μmol $CaCO_3$ cm^{-2} h^{-1}) were compared using an independent samples t-test after twelve weeks in ambient and high CO_2 conditions. There was no significant difference in light calcification rates between treatment conditions (t-test, p>0.05). Results from the independent samples t-tests indicated, however, that there were significant differences in dark calcification rates. *Orbicella faveolata* ambient (M = 0.154, SD = 0.13, n = 7) fragments calcified significantly more than those in high CO_2 (M = -0.030, SD = 0.09, n = 7), t(12) = -2.995, p = 0.0112, Fig. 2.2).
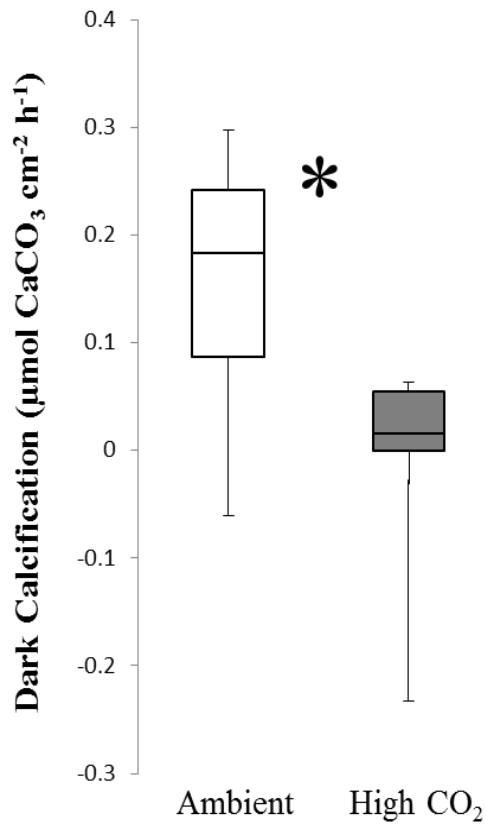
Figure 2.2: Average (mean ± SEM) of dark calcification (μmol $CaCO_3$ cm^{-2} h^{-1}) for *O. faveolata* (n=7) for twelve weeks. Asterisks represent significant differences between treatments determined using independent-samples t-test.

2.4   Discussion

Of the major environmental factors associated with the global distribution of coral reefs, such as temperature, light intensity, and seawater chemistry, most will be disrupted under conditions of global climate change (Kleypas et al. 2006). In this study seawater chemistry was manipulated to replicate near ambient (pCO_2 450 ppm) and predicted (pCO_2 1450 ppm) atmospheric values for 2100. *Orbicella faveolata* exhibited no significant difference in skeletal deposition rates under control and high CO_2 conditions; however, individual aragonite crystals in both adult and juvenile *O. faveolata* were statistically longer in the high CO_2 treatment. No significant differences were seen in photosynthesis or respiration rates. These results suggest that the addition of CO_2 may cause a shift in the overall energy budgets causing a modification of skeletal aragonite crystal structures and/or the organic matrix on which they are formed, rather than inhibiting skeletal crystal formation. Consequential to this energy shift, *Orbicella faveolata* may belong in the category of scleractinian corals that exhibit a low sensitivity to ocean acidification.

2.4.1   Net Calcification

The results of this study suggest that *Orbicella faveolata* may be able to acclimate to a more acidic ocean. Models based on physiochemical responses to ocean acidification (Ries 2011) and calcification kinetics in pH buffering (McCulloch et al. 2012) have identified two distinct classes of organisms exhibiting a low or high sensitivity to ocean acidification. *Orbicella faveolata* did not lose mass under low pH conditions and simultaneously displayed significantly enhanced crystal growth (Fig. 2.1). This calcification response to low pH, and therefore low Ω_{arag}, is consistent with   strong

internal pH regulation. Pacific coral species *Stylophora pistillata*, *Porites compressa*, and *Montipora verucosa* have been found to maintain ambient calcification rates over large ranges of Ω_{arag} conditions (Gattuso et al. 1998; Langdon and Atkinson 2005; Holcomb et al. 2014). These species may be directing a higher proportion of their energy budget to calcification (Pandolfi et al. 2011) or have a strong pH up-regulation mechanism in place (McCulloch et al. 2012). Through Ca^{2+}-ATPase antiporters in the calicodermis, corals remove two protons from the subcalicoblastic fluid in exchange for a calcium ion (Al-Horani et al. 2003; Cohen and McConnaughey 2003; Allemand et al. 2011). This process is energy expensive, but in the presence of excess ATP, corals can establish high internal aragonite saturation states despite significant changes in pH (Al-Horani et al. 2003). The energy required for this ion exchange and therefore calcification is derived predominately from photosynthesis; however, *Orbicella faveolata* did not experience a significant change in photosynthetic rate between treatment conditions. Energy expenditure during calcification is generally about one-third that produced from photosynthesis in *Symbiodinium* (Gattuso et al. 1999) but the extra energy required to up-regulate a pH change from 7.7 to 8.1 is less than 1% of the approximately 475 kJ mol^{-1} C^{-1} (McCulloch et al. 2012) generated through photosynthesis. Therefore, *O. faveolata* may not have needed to increase its energy budget in order to maintain net calcification rates. It is also possible that this species may draw from energy reserves to meet the new energy requirement (Schoepf et al. 2013). Towle et al. (2015) found that feeding rate and lipid content increased in corals experiencing OA conditions, and fed corals were able to maintain ambient growth rates at elevated CO_2. Corals that had been unfed, however, experienced significant decreases in growth with respect to fed conspecifics. Despite the lack of significant differences in growth rates between the control and experimental

32

groups, there was a large standard deviation for coral fragments grown in the high CO_2 environment. This could indicate a genotypic variation for *O. faveolata* in response to OA; restoration practices that are actively out planting this species would benefit from knowing which genets are less susceptible to future ocean conditions. While not evaluated in this experiment, overall health of coral reef systems may shift drastically with the compounding effects of increasing thermal stress from global warming and local environmental impacts (Pandolfi et al. 2011; McCulloch et al. 2012; Cumbo et al. 2013; Schoepf et al. 2013).

2.4.2 Physiology

Stony corals, the framework builders of coral reefs globally, are highly susceptible to ocean acidification as their calcium carbonate skeleton represents the highest proportion of their mass (Knoll et al. 2007). However, there are multiple partners that make up the coral holobiont, all of which interact at the most basic metabolic level (Horwitz et al. 2015). Included in the coral holobiont are external and internal microbes, endolithic algae, bioeroders, and dinoflagellates. *Symbiodinium*, the symbiotic dinoflagellate present in zooxanthellate corals, utilize bicarbonate (HCO_3^-) instead of $CO_{2(aq)}$, as the primary source for photosynthesis (Kleypas et al. 2006; Brading et al. 2013). Bicarbonate concentrations will increase about 14% under doubled CO_2 conditions predicted for 2100 (Kleypas et al. 2006). The interaction of these organisms includes exchanging energy and nutrient-rich compounds; hence it is necessary to consider the role of *Symbiodinium* energy acquisition through photosynthesis when examining the coral host's physiological calcification process. The relationship between photosynthesis and calcification in benthic calcifiers is poorly understood (Kleypas et al. 2006). Calcification rates can be enhanced by photosynthesis (Gattuso et al. 1999), but

the stimulating mechanism remains poorly known (Cohen and McConnaughey 2003). Many studies have reported net photosynthetic rates of corals displaying either no or a slight increase in response to increased pCO_2 (Langdon and Atkinson 2005; Schneider and Erez 2006; Anthony et al. 2008). In this study, there was no significant impact of ocean acidification on oxygen production, indicating that the photosynthetic benefit of an increased CO_2 supply may be overridden by the disruption of photophysiological processes (Anthony et al. 2008), or that photosynthetic rates are not DIC-limited. Though higher concentrations of bicarbonate are present under OA conditions, low pH may interfere with the pathway for CO_2 accumulation thereby directly affecting the ability of the individual symbionts to fix carbon (Anthony et al. 2008). It is also unclear if the insignificant impact of OA on photosynthesis and respiration is an acclimation response or if excess CO_2 does not impact the holobiont in this study. There is a gap in research on the molecular and biochemical pathways of the photosynthesis-calcification relationship. Understanding this relationship is required before the effect of environmental changes on coral physiology can be deciphered.

2.4.3   Electron Microscopy

Calcification in multiple life stages plays a critical role in survival, but almost all studies of CO_2 effects on calcification have focused on adult organisms (Kleypas et al. 2006). Understanding the effects of OA on calcification in a species' adults and newly settled recruits can help reveal true impacts across individuals' many life stages. For example, slowed juvenile growth may result in more time spent in the juvenile stage, therefore lengthening the period in which corals are not sexually reproductive. In combination with adult loss, population structures would shift toward smaller class sizes, decreasing effective population sizes and population fecundity (Albright and Langdon

34

2011). The results from this experiment show a similar response in skeletal structure in adults and newly settled *O. faveolata* recruits in each of the treatment conditions. In high CO_2 (>1450 ppm) treatment seawater, this species displayed longer crystal growth (Fig. 2.2), indicating the ability to nucleate and grow crystals more rapidly than corals grown in the ambient condition. This response was consistent between different genets. Crystals secreted in corals from the high CO_2 treatment displayed the characteristic thin, blade-like structure, associated with day time growth (Cohen and Holcomb 2009). In contrast to this study, the skeleton accreted from *Favia fragum* spat revealed a reduced length to width ratio as saturation state decreased, though all corals reared at various levels of aragonite saturation conditions, even to the point of undersaturation, were able to accrete and maintain aragonite crystals (Cohen et al. 2009). Venn et al. (2013) found that new crystal growth in *Stylophora pistillata*, as measured by changes in cross-sectional area, for corals maintained at pHs 8.0, 7.8, and 7.4 showed no significant difference. These results, along with our data, imply that there is a physiological resilience across distinctly different species that may alleviate the stress of ocean acidification in order to achieve present levels of calcification. Although the results support the concept that specific coral species up-regulate pH at the site of calcification resulting in nucleation of new skeletal crystals, the variability in crystal structure implies that this may result in a shift in the structural density of the coral (Drenkard et al. 2013). Other studies have found skeletal integrity impairments under OA conditions for Caribbean species *F. fragum* and *P. astreoides* (Cohen et al. 2009; de Putron et al. 2011), which may further reduce the resilience of the already degraded population (Enochs et al. 2014; Holcomb et al. 2014).

Enhanced extracellular organic matrix gene expression was documented for *Acropora millepora* under high CO_2 (1000 ppm) conditions (Moya et al. 2012). This

response was quite complex; genetically distinct individuals responded differently to the number and location of skeletal organic matrix genes they up-regulated or down-regulated. This altered expression and overall disturbance of the skeletal organic matrix which could explain the variability in size, shape, and orientation of the aragonite crystals observed in this and other experiments (Cohen et al. 2009; Cohen and Holcomb 2009; Moya et al. 2012; Drenkard et al. 2013; Venn et al. 2013).

2.4.4   Conclusions

Although *Orbicella faveolata* was recently added to the IUCN threatened species list, this species appears to be quite resilient in a more acidic environment. This observation is based on the results that *O. faveolata* did not experience any growth deficit under high CO_2 conditions and crystal structure of recently nucleated skeletal material was statistically longer in the low pH treatment (Cohen and Holcomb 2009). This crystal length trend existed across generational boundaries as the recently settled spat also displayed longer crystals in the high CO_2 treatment (Fig. 2.1).

Any event that leads to the reduction of primary productivity, such as the prevalence of disease, can potentially impact coral calcification (Wild et al. 2011). Black band disease (BBD) has a widespread distribution throughout the Caribbean, the Red Sea, the Indo-Pacific, and the Great Barrier Reef, preferentially infecting large, reef-building corals (Richardson 2004). It is one of the more complex and destructive coral diseases known, lysing tissue as the band of cyanobacteria progress over the surface of the infected coral. The cyanobacteria present within the BBD mat have been shown with scanning electron microscopy (SEM) to bore through the $CaCO_3$ coral skeleton at the site of infection and to penetrate the coral tissue, contributing to tissue lysis (Miller et al. 2011; Miller and Richardson 2011). To my knowledge, there have been no studies

completed on the impact of BBD on coral calcification directly. Although the *Orbicella faveolata* adults were exposed to BBD prior to this experiment, care was taken to remove all diseased areas as well as a 1" margin into the healthy tissue prior to taking any physiological readings. Aeby et al. (2015) showed that removing the diseased margin *in situ* lead to a significant reduction in disease prevalence for *Montipora sp.* in Hawaii. Additionally, there was no evidence of cyanobacteria or other components of BBD in the transmission electron micrographs of this species.

The response of coral calcification to ocean acidification is ultimately dictated by the limits of coral physiology to acclimate or adapt to a more acidic ocean rather than just kinetics alone (McCulloch et al. 2012). pCO$_2$-tolerant corals have been characterized by an increased ability to acclimatize to ocean acidification, e.g. by maintaining net calcification (Strahl et al. 2015). Robust corals are more likely to persist for longer in a future high pCO$_2$ world than those unable to acclimatize. Although many studies have evaluated the responses of adult corals (Anthony et al. 2008; Marubini et al. 2008; Holcomb et al. 2012; Moya et al. 2012; Schoefp et al. 2013; Enochs et al. 2014; Holcomb et al. 2014), juveniles (de Putron et al. 2011; Drenkard et al. 2013) or larval physiology and settlement (Albright et al. 2008; Cohen et al. 2009; Albright et al. 2010; Albright and Langdon 2011; Cumbo et al. 2013) under ocean acidification conditions, there still remains a large gap in knowledge as many projects have included just a few species. It is crucial to continue understanding how OA will influence all coral reef organisms as their interactions create this ecosystem. Here I found that elevated pCO$_2$ had no significant effect on average growth rates or physiology parameters. I also found a distinct quantitative difference in the skeletal crystals produced in ambient versus high CO$_2$ seawater, a relationship that remained between life stages. This seemingly positive

response may have drawbacks in the overall energy budget for the coral. If in fact this species is directing a higher proportion of their energy budget to calcification there will be less resources available for critical functions such as gamete production and immune system response. Further studies are needed to uncover the mechanism by which *O. faveolata* is able to lengthen its crystal structure and determine the impacts on other parameters.

Chapter 3

Effects of ocean acidification on growth and microcalcification in reef building

Caribbean species

3.1   Introduction

The seawater changes due to rapidly rising anthropogenic addition of carbon dioxide into the atmosphere predicted for the end of the century present major challenges for calcifying organisms. Over 25% of CO_2 produced since the Industrial Revolution has been absorbed by the oceans (Calderia and Wicket 2003; Sabine et al. 2004; Sponberg 2007). Although mitigating the effects of global warming, the 'oceanic sink' (Sabine et al. 2004) of carbon dioxide is expected to result in a 0.4 pH unit decrease of the surface oceans by the end of the century (Calderia and Wicket 2003; Raven et al. 2005; IPCC 2013), causing the issue of ocean acidification. For the past thirty years, the rate of net carbon dioxide emission into the atmosphere has been 1.79 ppm year^{-1} (IPCC 2013). This present value is two to three orders of magnitude higher than rates from over the past 420,000 years (Hoegh-Guldberg et al. 2007; Knoll et al. 2007). The associated changes in oceanic pH are developing 100 times faster than any records of the past hundreds of millennia (Calderia and Wicket 2003; Raven et al. 2005). Yet, little is known about how long term seawater acidification, increased carbon dioxide partial pressure, and the pH associated changes to ocean chemistry will influence marine organisms (Turley et al. 2006).

For scleractinian corals, biogenic calcification occurs within a physiologically controlled environment (Al-Horani et al. 2003; Cohen and McConnaughey 2003; Venn et al. 2011; McCulloch et al. 2012; Holcomb et al. 2014). Corals raise the pH of an extracellular calcifying fluid in a semi-isolated space during active calcification in order

to promote dissolved organic carbon (DIC) components to shift toward carbonate (Al-Horani et al. 2003; Holcomb et al. 2014). Net calcification has typically been shown to decline after exposure to climate stressors such as ocean acidification (Langdon and Atkinson 2005; Schneider and Erez 2006). The magnitude of the decline differs among s species and is highly variable (Anthony et al. 2008; Ries et al. 2009, de Putron et al. 2011; Pandolfi et al. 2011; Silbiger and Donahue 2015). Recent work has found that, although net calcification is declining, corals are still secreting new skeletal material (Cohen et al. 2009; McCulloch et al. 2012; Enochs et al. 2014; Holcomb et al. 2014; Tambutté et al. 2015). Successful calcification is dependent on an organism's ability to achieve supersaturation in their calcifying fluid; this process is limited by energy requirements (McCulloch et al. 2012). Future success of marine calcifying organisms in a high CO_2 environment could be based on an individual's ability to overcome this limitation (Cohen et al. 2009).

As the rain forests of the ocean, coral reefs are among the most diverse ecosystems on the planet due to the structurally complex calcium carbonate foundation of coral reef ecosystems (Knoll et al. 2007). This three-dimensional structure is at risk to be degraded by ocean acidification (Fabricius et al. 2011; Silbiger and Donahue 2015). Nearly one fifth of the world's coral reefs have gone extinct and another 30% are expected to be lost in the coming decades unless the effects of global climate change are mediated (Vernon et al. 2009; Pandolfi et al. 2011). There have been several studies that evaluated the responses of adult corals (Anthony et al. 2008; Marubini et al. 2008; Holcomb et al. 2012; Moya et al. 2012; Schoefp et al. 2013; Enochs et al. 2014; Holcomb et al. 2014; Tambutté et al. 2015), juveniles (de Putron et al. 2011; Drenkard et al. 2013), or larval physiology and settlement (Albright et al. 2008; Cohen et al. 2009; Albright et

al. 2010; Albright and Langdon 2011; Cumbo et al. 2013) under ocean acidification conditions. However, there still remains a gap in knowledge as many projects have included only a few species.

In this study comparison of the effects of high CO_2 on calcification was examined by raising adult *Dichocoenia stokesi* and *Montastraea cavernosa* fragments in a high CO_2 environment based on the RCP8.5 IPCC scenario. RCP8.5 represents 'business as usual' where there is strong economic development for the rest of this century, driven primarily by dependence on fossil fuels (IPCC 2013). Investigation of the effects of ocean acidification on two key physiological processes was made and electron microscopy utilized for ultrastructural examination of coral skeletal structure. The impact of increased pCO_2 on net calcification through buoyant weights and alkalinity anomaly were examined. Productivity, which is expected to be influenced by an altered carbonate chemistry (Anthony et al. 2008), was documented as oxygen production and consumption via photosynthesis and respiration. Using SEM, the crystal structures of newly deposited calcium carbonate were compared across treatment conditions for each species. *Dichocoenia stokesi* and *Montastraea cavernosa* represent some of the most common and major framework building corals in the Florida Reef Tract.

Examined is the effect of lowered ocean pH, reduced carbonate concentrations, and high pCO_2 on the microcalcification of corals using two species to address the following questions: Do morphometrically distinct hermatypic coral species: *M. cavernosa* and *D. stokesi* respond differently to ocean acidification? Do *M. cavernosa* and *D. stokesi* acclimate or change their response over time under persistent exposure to high pCO_2 conditions*?

3.2   Methods

3.2.1   *Coral collection*

Montastraea cavernosa and *Dichocoenia stokesi* are two mounding hermatypic scleractinian corals commonly found on fore-reef habitats and represent two of the crucial framework builders on Caribbean coral reefs. Four *M. cavernosa* and *D. stokesi* colonies were collected at 7-10 m depth from BC1 reef off Ft. Lauderdale, FL on August 16th, 2014 using a hammer and chisel. *Dichocoenia stokesi* (Milne, Edwards, and Haime 1848) is among the most common coral in the Florida Keys and Dry Tortugas, with population abundance estimates close to 100 million colonies in 2005 (Miller et al. 2013). *Dichocoenia stokesi* is hypothesized to be robust and may be well suited to acclimate to lowered oceanic pH values induced by high atmospheric carbon dioxide values given its large population numbers, broad distribution among multiple habitat types, and high relative abundance among all corals in the Florida Reef Tract (Miller et al. 2013). The reef coral *Montastraea cavernosa* is a common, widely distributed species, easily identified by its distinct large fleshy polyps and large mounding structure (Budd et al. 2011). Water depth distribution extends from 0.5 to 95 m. Highest occurrences have been found at intermediate to deep reef depths of 10–60 m (Goreau 1959; Goreau and Wells 1967). This species geographic distribution extends across the Caribbean, as far north as Bermuda in the North Atlantic, and to Brazil in the South Atlantic and the Gulf of Guinea in the Eastern Atlantic (Laborel 1974; Sterrer 1986); such a wide distribution suggests that *M. cavernosa* has an evolutionary predisposition to acclimate to less than favorable environmental conditions.

Colonies were transported to Mote Marine Laboratory (MML), Sarasota, FL, in seawater saturated bubble wrap, where they were allowed to acclimate in the flow

through system (OASys) for two days. Corals were held in 20 L aquaria supplied with sand bed filtered (30 μm) Sarasota Bay seawater (flow rate 75 mL min^{-1}) at a salinity of 35 ppt, temperature of 25 °C, and irradiance of 80 μmol photons m^{-2} s^{-1} on a 12h light/dark cycle (T5 fluorescent actinic and daylight bulbs). Eight 4 cm^2 fragments were removed from each colony using a 7" wet tile saw and placed in separate flow-through tanks (n=8). By using fragments from multiple colonies of each species, this experiment can evaluate a species level response to ocean acidification.

3.2.2   Experimental Design

The experimental facility consisted of 8 flow-through aquaria (20 liters) under a 12:12 hour light/dark regime (T5 Fluorescent Actinic pink and blue daylights), receiving sand bed filtered reef seawater (30 μm) from two temperature-controlled (Delta Star in-line water chiller, Aqua Logic, Inc., Hydortheo submersible, 50-100 watt heaters) CO_2 mixing tanks (Fig. 3.1). All experimental tanks were kept at a flow rate close to 75 mL/min to allow for a complete turnover rate of approximately four hours. Levels of acidification were regulated through a pH stat system (Apex Neptune Jr. Controller with pH probe module) set to pH target values of 8.10 and 7.70, corresponding to CO_2 concentrations of 450 ppm and 1450 ppm for the ambient and high CO_2 dosing regimens, respectively (Table 2). pH was measured on the NBS scale using Lab Grade Neptune Systems pH probes, each connected to the logger/controller unit via a Neptune Systems Apex controller. The experimental CO_2 environments were chosen to simulate the current atmospheric CO_2 levels and the RCP8.5 scenario presented in the International Panel on Climate Change (IPCC) Fifth Assessment Report (AR5), with year 2100 pCO$_2$ (ppm) >1370 ppm (IPCC, 2013; Moss et al. 2010). Daily measurements of pH (Mettler Toledo SevenGo pro), temperature (EcoSense EC300A), and salinity (EcoSense EC300A) were

compiled with weekly total alkalinity (TA) to determine the distribution of carbon species and aragonite saturation state for all treatments (Table 3.1) using the program CO2SYS (Lewis and Wallace 1998). Sample collection and storage for TA was done in 120 mL borosilicate bottles that were cleaned with 10% HCl and rinsed three times with nanopure water. TA was measured using a modification of the open-cell titration method (Dickson et al. 2007, SOP 3b) on a Metrohm 916 Ti-Touch automated titrator using 0.05M HCl in 0.6M NaCl for 32 g seawater samples. All TA data was verified for accuracy using certified reference material (CRM) seawater from the Dickson Lab at Scripps Institute (CRM # 137). CO2SYS was run using the K1K2 apparent equilibrium constants from Mehrback (1973) and refit by Dickson and Millero (1987), HSO_4^- dissociation constants were taken from Uppstrom (1974) and Dickson (1990), and pH was on the NBS scale.
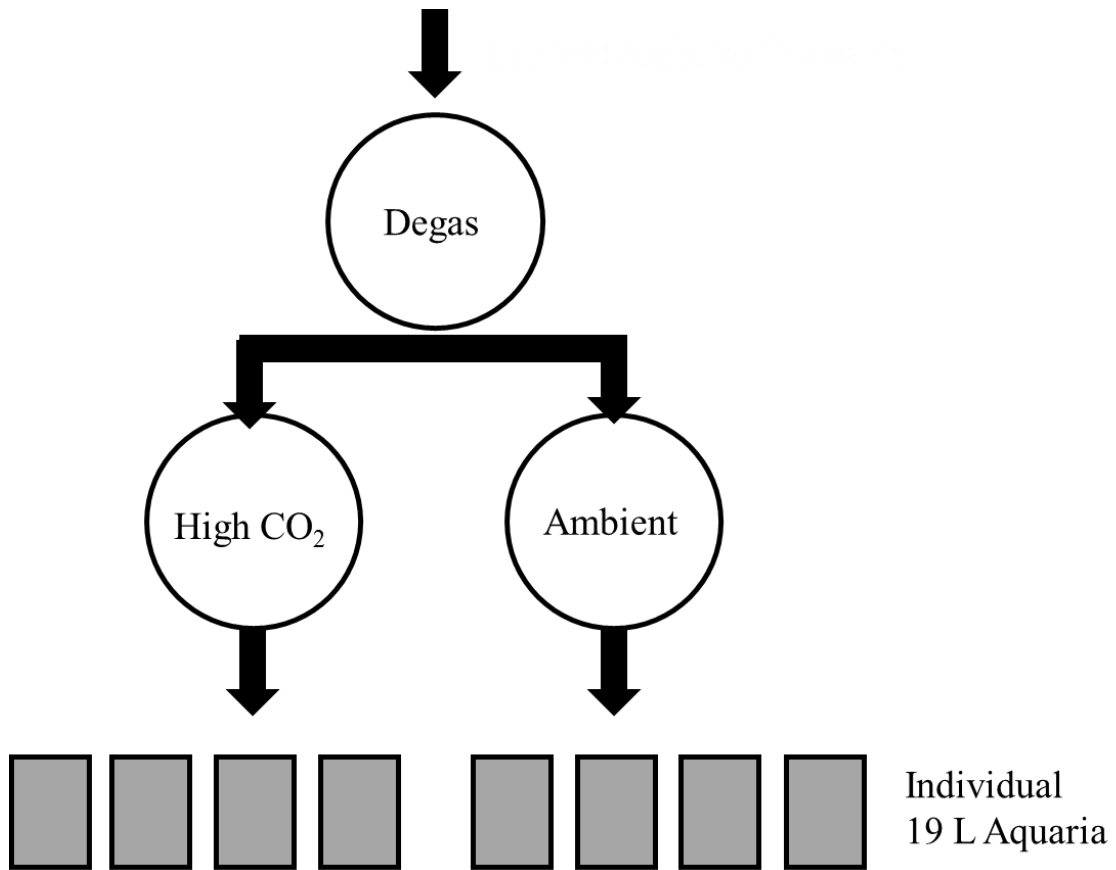
Figure 3.1: A schematic of the microcosm system at Mote Marine Laboratory's OASys lab. Ambient seawater is pumped into the system from Sarasota Bay, where it is treated by ozonation and sand bed filtration to remove particles in excess of 30 μm. The 65 gallon degas tank tempers the pH of incoming seawater through aeration from an outdoor air pump connected to two large air stones sitting at the bottom of the tank. Water is transferred from the degassing tank through a bulkhead at the bottom to an external pump to each of the treatment header tanks. Both ambient and high CO_2 tanks contain a pH probe, temperature probe, and circulation pump. The high CO_2 tank also contains a CO_2 gas line, which runs to a CO_2 tank and electronic regulator to manipulate pCO_2. When the pH of this tank rises above a 7.7 point programed into the apex controller (Neptune Systems), power to the electronic regulator is turned on and pure CO_2 is allowed into the acidified tank. Water flows through a bulkhead at the bottom of each of the header tanks and into a 1 inch supply manifold. Flow is controlled in each individual aquarium.

Table 3.1: Means (± standard errors) of all measured parameters by treatment header tank. pCO_2, HCO_3^-, CO_3^{2-},

CO_2, DIC, and Ωarag were l calculated from measured TA and pH samples using CO2SYS

Header Tank	Temperature (°C)	Salinity (psu)	pH (NBS)	Alkalinity (μmol kg^{-1})	pCO_2 (ppm)	DIC (μmol kg^{-1})	[CO_2] (μmol kg^{-1})	[HCO_3^-] (μmol kg^{-1})	[CO_3^{2-}] (μmol kg^{-1})	Ωarag
Ambient	25.77±0.07	34.96±0.04	8.14 ± 0.002	2441 ± 5.38	465 ±5.52	2126±8.48	12.4±0.21	1889±10.4	224.5±2.75	3.6 ± 0.05
High CO_2	26.35±0.06	34.98±0.05	7.65 ± 0.003	2443 ± 5.35	1451 ± 6.51	2333±5.71	38.1±0.27	2195±5.68	99.2±0.81	1.6 ± 0.01

3.2.3 Buoyant weight

Buoyant weights were measured prior to the start of the experiment and after one, three, and fifteen weeks in the treatment conditions using an Ohaus Adventure Pro analytical balance; aquaria were held at 25.0 ± 0.5 °C throughout this period. Temperature and salinity were recorded for every weighing to calculate seawater density. Weights were measured as described by Davies (1989). Calcification rate was quantified from the difference in buoyant wet weights between the week measured and the initial mass (week 0). Data was normalized to tissue surface area and expressed as mg $CaCO_3$ cm^{-2} d^{-1}.

3.2.4 Physiology

Productivity was measured for *D. stokesi* and *M. cavernosa* fragments after one, three, and fifteen weeks in the experimental conditions. Four fragments of each species and treatment were placed into one of four sealed, recirculating respirometry chambers and agitated using a magnetic stirrer. Physiology measurements were performed at the same temperature and seawater chemistry as the experimental tanks. Photosynthesis was measured as the oxygen production for one hour under controlled artificial lighting (T9 fluorescent and 4 LED strip lights) matching the daytime OASys irradiances of 80 μmol photons m^{-2} s^{-1} and respiration measurements as oxygen consumption during a one hour

period in complete darkness. Each chamber was connected to a high-precision fiber-optic oxygen meter and logging system (FirestingO2, Pyro Science). Before measurements were taken, sensors were calibrated against air-saturated seawater. Oxygen fluxes of all specimens were estimated by regressing oxygen data against time and normalized to tissue surface area determined from geometric analyses of digital photographs (ImageJ, NIH).

3.2.5 Alkalinity Anomaly

For each light and dark hour in the respirometry chambers, a water sample was removed from the chamber and analyzed for total alkalinity using a modification of the open-cell titration method (Dickson et al. 2007, SOP 3b) on a Metrohm 916 Ti-Touch automated titrator using 0.05 M HCl in 0.6 M NaCl titrant for 32 g seawater samples. Water samples were filtered (0.2μm membrane filters) prior to analysis. This alkalinity anomaly method (Andersson et al. 2009; Silbiger and Donahue 2015) calculates net calcification from changes in TA. Samples that could not be run immediately were stored in a 2°C refrigerator and processed within a week. Calcification was determined using the alkalinity anomaly method (Smith and Key 1975; Riebesell et al. 2010). In this study calcification rates were normalized to surface area.

3.2.6 Electron Microscopy

At weeks 1, 3, and 15 a coral sub-sample was removed from each treatment condition. An approximate 2 cm^2 section of tissue and skeleton was removed from the adults using a dremel tool (Dremel 200) and placed in a 50% NaClO solution and thoroughly rinsed in fresh water in preparation for scanning electron microscopy (SEM). Additional coral fragments, cut for a maximum surface area of 1 cm^2 were prepared for TEM analysis by immersing them into 2% glutaraldehyde in 0.05 M sodium cacodylate-

buffered filtered seawater immediately after removal from experimental aquaria. In the laboratory, the glutaraldehyde fixative was refreshed, and fragments were transferred to and rinsed in 0.05 M sodium cacodylate filtered seawater buffer (3× for 10 min each), and post fixed in 1% osmium tetroxide in buffer for 30 min. After an additional 3 buffer washes, the fragments were dehydrated in a graded series of ethanol, with a final concentration of 100%. Small sub fragments were created using the larger TEM pieces to remove most of the calcium carbonate. The coral fragments used for SEM were mounted on carbon adhesive-covered aluminum stubs and coated with palladium. Samples were imaged in an FEI XL-30 ESEM/SEM fitted with an Oxford EDS system. For TEM analysis, the calcified sub fragments in 100% ethanol were embedded in Spurr© embedding resin. A Sorval MT-2 ultramicrotome fitted with a diamond knife was used to cut sections of the coral and skeleton embedded in the blocks. Sections were placed on copper grids and left unstained. Since calcified material was sectioned, uranyl acetate stain was not used; an acidic stain would dissolve the sectioned calcium carbonate skeleton, which was a subject of this study. Sections were imaged utilizing a CM-20 Philips TEM fitted with a Gatan digital camera in the EM Core Facility at the University Of Miami Miller School Of Medicine.

After coating with a 20nm layer of Pd in a plasma sputter coater, skeleton fragments were examined at several magnifications in the SEM. The columella was targeted to image the crystal structure of newly calcified skeleton. Images were analyzed in ImageJ (NIH) to quantify the length of the crystals produced by each species and time period. TEM images were examined to gain information about the cellular process of calcification under each treatment. Areas observed include the epidermis, gastrodermis

and included zooxanthellae, as well as the calicoderm, to assess potential effects on coral tissue and calcification.

3.2.7 Statistical Analysis

The software program JMP was used to examine independent and interaction relationships between treatment variables. Individual aquariums were analyzed to verify that there were no differences between treatment tanks. After confirming non-significant difference between tanks, data was pooled in subsequent analyses and specimens were used as replicates. Net calcification (buoyant weight), crystal length, oxygen production and consumption from physiology parameters and calcification data from alkalinity anomaly for all three species were evaluated to compare CO_2 treatments (ambient, pH_{NBS} 8.14, pCO_2 450 ppm and high CO_2, pH_{NBS} 7.71, pCO_2 1450 ppm) and species-specific responses. Each species response to these variables after fifteen weeks to CO_2 treatments were tested using an independent samples t-test. To compare data that was collected across various time points, repeated measures ANOVA was run by species with treatment condition at the model effect. For data that violated Mauchly's Test of Sphericity, a correction was used; the Greenhouse-Geisser correction was applied if the estimated epsilon (ε) is less than 0.75 and the Huynd-Feldt correction was used if the estimated epsilon (ε) is greater than 0.75. When there were significant differences in the interaction of time and treatment, an independent one-way ANOVA was used to examine where the differences were. Data were tested for variance homogeneity using Levene's test and normality using the Shapiro-Wilk test. Kruskal-Wallis and Wilcoxon tests were run for non-normal sample sets for the t-tests and one-way ANOVAs respectively.

3.3   Results

3.3.1   Buoyant Weight

Independent-samples t-tests were run to compare mean net calcification (mg $CaCO_3 \, cm^{-2} \, d^{-1}$) between the treatment conditions for each species over the experimental period. *Dichocoenia stokesi* fragments grown in high CO_2 seawater (M = -0.532, SD = 0.15, n = 7) [t(11) = -3.550, p = 0.0046](Fig. 3.2a) experienced a statistically significant 800% decrease in growth rate compared to those grown in ambient seawater (M = 0.073, SD = 0.42, n = 6).. *Montastraea cavernosa* exhibited a 343% decrease in growth rate after fifteen weeks of exposure. Fragments in high CO_2 (M = -0.310, SD = 0.13, n = 6) [t(12) = 2.554, p = 0.0253] (Fig. 3.2a) also displayed a significant decrease in growth from those in the ambient treatment (M = -0.070, SD = 0.20, n = 8)). To compare buoyant weights for *D. stokesi* and *M. cavernosa* over time, a repeated measures ANOVA was run with treatment as the model effect. There were no significant differences in net calcification across time for *Dichocoenia stokesi* fragments after fifteen weeks between time points sampled or treatment conditions (p>0.05). Additionally, there was no interaction between treatment and time, indicating that the fragments in each CO_2 condition did not differ in their response over time (p>0.05) (Fig. 3.3a). *Montastraea cavernosa* fragments, however, exhibited a significant treatment effect [F(1,12) = 10.0668, p = 0.0080], time [F(2,11) = 16.9989, p = 0.0004] and the interaction of both variables [F(2,11) = 7.6092, p = 0.0084]. To find where *M. cavernosa* displayed differences, a one-way between subjects ANOVA was run for each treatment condition. Where assumptions were not met, the Kruskal-Wallis test was used. *Montastraea cavernosa* fragments in the ambient condition displayed a significant increase in growth rate over time [F(2,33) = 7.1427, p = 0.0026]. Post hoc comparisons using the Tukey

HSD test indicated a significant increase in growth rate (mg $CaCO_3$ cm^{-2} d^{-1}) in fragments from one week of exposure (M = -1.856, SD = 1.81, n = 16) to those after three (M = -0.228, SD = 0.70, n = 12) and fifteen weeks (M = -0.070, SD = 0.20, n = 8), all in ambient seawater (Fig. 3.3c). In contrast, *Montastraea cavernosa* fragments in the high CO_2 condition did not experience any significant change in growth rate over time (one-way ANOVA, p>0.05).

3.3.2 Crystal Length

Independent-samples t-tests were conducted to compare the lengths of recently nucleated crystals for *D. stokesi* and *M. cavernosa* in ambient and high CO_2 conditions. Data was derived from scanning electron micrographs of the columella region for each treatment at 20,000x magnification (Fig. 3.2c). The nonparametric Wilcoxon test was used for data that did not meet the statistical assumptions for the independent-samples t-test. In both species there was a significant difference in crystal length in each treatment during the final sampling period (Table 3.2, Fig. 3.2b). The results show that the simulation of future ocean acidification conditions led to a significant reduction in crystal length.

Table 3.2: Results of t-test and descriptive statistics for crystal length by treatment.

	Ambient			High CO_2					
	M	SD	n	M	SD	N	t/Chi^2	df	p
D. stokesi	2.836	0.17	10	1.185	0.17	10	-6.846	18	<.0001
M. cavernosa*	0.681	0.21	10	0.288	0.07	10	13.7303	1	0.0002

*Data run using Wilcoxon test
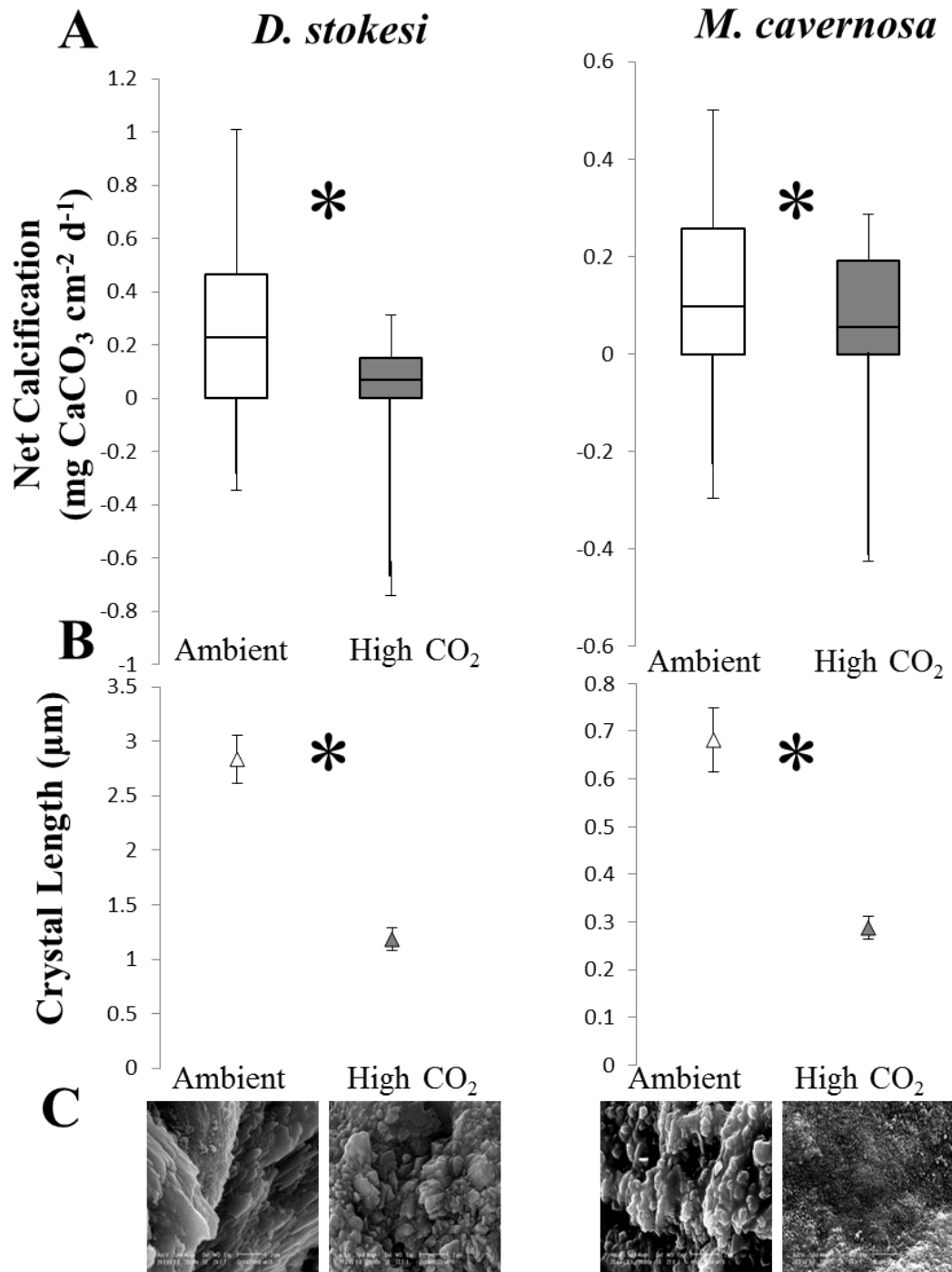
Figure 3.2: Box plot diagrams of net calcification via buoyant weight (mg $CaCO_3$ cm^{-2} h^{-1}) (A) and average (mean ± SEM) of crystal length (µm) (B) determined from scanning electron micrographs (C) for *D. stokesi* and *M. cavernosa* fragments under ambient (pH_{NBS} 8.14) and high CO_2 (pH_{NBS} 7.71) conditions. Asterisks represent significant differences between treatments, t-test p<0.05. All scale bars are 2 µm.

To compare crystal length in *D. stokesi* and *M. cavernosa* over time, a one-way between subjects ANOVA was run for each treatment condition. Where assumptions were not met, the Kruskal-Wallis test was run. A repeated measures ANOVA was not used as each time point utilized different fragments and therefore the data do not meet the assumption of dependence. There were no significant differences in crystal length over time for *D. stokesi* fragments grown in either ambient or high CO_2 treatments (Kruskal-Wallis, $p>0.05$). A one-way ANOVA revealed that there was a significant change in crystal length during the fifteen week experimental period in *M. cavernosa* fragments grown in the ambient seawater [$F(2,30) = 94.0202$, $p < 0.0001$]. Post hoc comparisons using the Tukey HSD test indicated significant differences between crystal lengths (µm) between those reared for three weeks (M = 2.640, SD = 0.44, n = 10) compared to those after one (M = 0.858, SD = 0.38, n = 13) or fifteen weeks (M = 0.681, SD = 0.21, n = 10) (Fig. 3.3d). *Montastraea cavernosa* fragments in the high CO_2 condition displayed a significant fluctuation in crystal length over time as well [$H(2) = 11.8347$, $p = 0.0027$]. Both ambient and high CO_2 fragments for *M. cavernosa* showed a sharp rise in crystal length at week three, which was not observed after fifteen weeks in the experimental system.
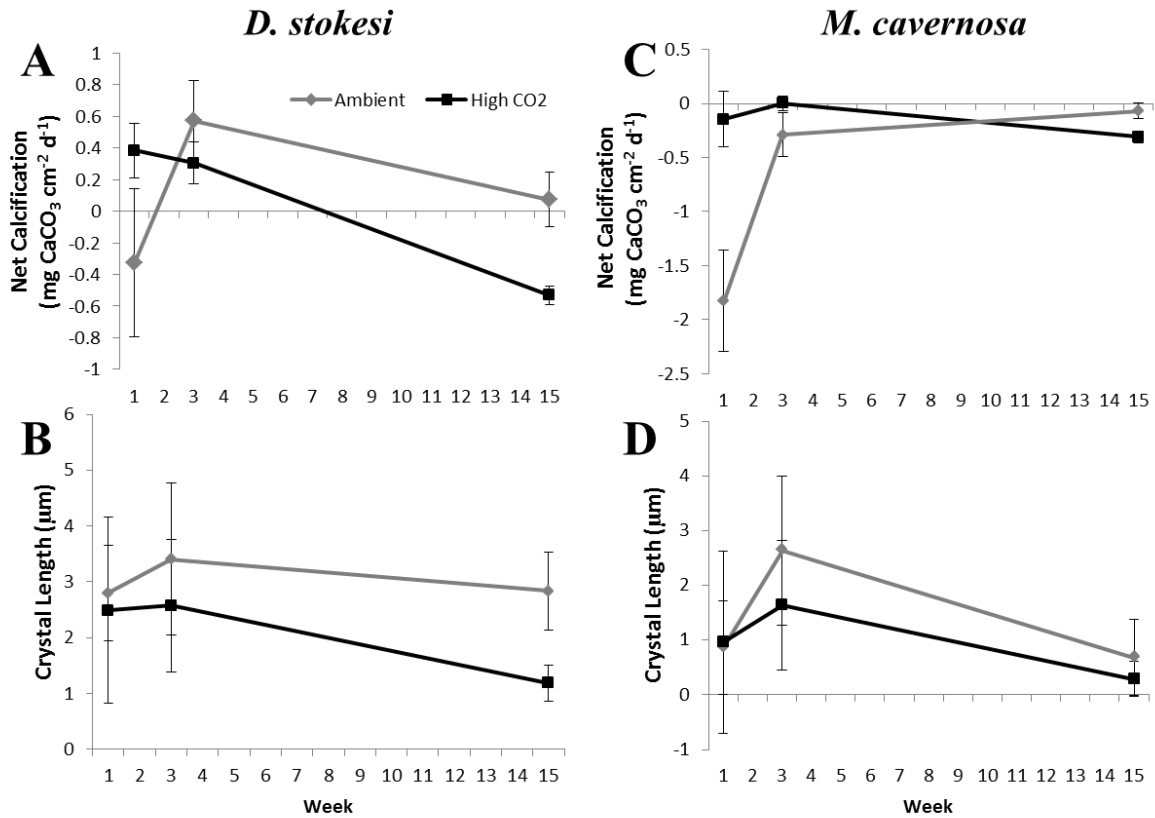
Figure 3.3: Average (mean ± SEM) net calcification (mg $CaCO_3$ cm^{-2} d^{-1}) via buoyant weight (top row) and average (mean ± SEM) crystal length (μm) (bottom row) for *D. stokesi* (A,B) and *M. cavernosa* (C,D) fragments grown under ambient (pH_{NBS} 8.14) and high CO_2 (pH_{NBS} 7.71) conditions across the three sampling periods. Data was analyzed using a one-way ANOVA or a Kruskal-Wallis test where assumptions were not met.

3.3.3 Physiology

An independent samples t-test was performed to compare each of the *D. stokesi* and *M. cavernosa* fragments mean photosynthetic and respiration rates after fifteen weeks in ambient or high CO_2 conditions. There was no significant effect of treatment for each of the species during the final sampling period on oxygen production or consumption through photosynthesis and respiration (t-test, $p>0.05$).

To investigate if there were changes in the mean photosynthetic rate over time, a repeated measures ANOVA was run by species with the effect of treatment. Where the assumption of sphericity was not met, the Greenhouse-Geisser correction was used. There were no significant differences in oxygen production over time in *Dichocoenia stokesi* fragments after fifteen weeks between time points sampled or treatment conditions (G-G, $p>0.05$). Additionally, there was no interaction between treatment and time, indicating that the fragments in each CO_2 condition did not differ in their response over time (G-G, $p>0.05$) (Fig. 3.4a). *Montastraea cavernosa* fragments had a significant effect of treatment [$F(1,5) = 8.7985$, $p = 0.0313$] and time [$F(2,11) = 16.9989$, $p = 0.0004$] on mean photosynthetic rates, but not the interaction of both. These results indicate that increased carbon dioxide concentrations may have a positive impact on zooxanthellate productivity, albeit a temporary one, but this is a coral species specific response and may be related to the *Symbiodium sp.* clade present.

To investigate if there were changes in mean respiration rates over time, a repeated measures ANOVA was run by species with the effect of treatment. Where the assumption of sphericity was not met, the Greenhouse-Geisser correction was used. There were no significant differences in oxygen consumption over time in *Dichocoenia stokesi* fragments after fifteen weeks between time points sampled or treatment

conditions (G-G, p>0.05). Additionally, there was no interaction between treatment and time, indicating that the fragments in each CO_2 condition did not differ in their response over time (G-G, p>0.05) (Fig. 3.4b). *Montastraea cavernosa* fragments had a significant effect over time [$F(2,11) = 16.9989$, p = 0.0004] only. *Montastraea cavernosa* fragments displayed a significant reduction over time in respiration rate, regardless of treatment. There was a significant drop in oxygen consumption (μmol O_2 cm^{-2} h^{-1}) for *M. cavernosa* ambient fragments from week one (M = -0.022, SD = 0.002, n = 4) to weeks three (M = -0.014, SD = 0.003, n = 4) and fifteen (M = -0.011, SD = 0.003, n = 8) in (Fig. 3.4d). Similarly, there were significant reductions in oxygen production over each measured time point for *M. cavernosa* fragments grown in the high CO_2 treatment from week one (M = -0.021, SD = 0.005, n = 4) to week fifteen weeks of exposure (M = -0.011, SD = 0.003, n = 5) in high CO_2 conditions (Fig. 3.4d). Given the similarity of these relationships, it is clear that a factor other than $p$$CO_2$ is influencing respiration rates, such as reduced stress over time due to acclimation to new seawater.

Figure 3.4: Average (mean ± SEM) oxygen production (µmol O_2 cm^{-2} h^{-1}) from photosynthesis (top row) and consumption via respiration (bottom row) for *D. stokesi* (A,B) and *M. cavernosa* (C,D) under ambient (pH$_{NBS}$ 8.14) and high CO_2 (pH$_{NBS}$ 7.71) treatments across the three sampling periods. Data was analyzed using a one-way ANOVA or a Kruskal-Wallis test where assumptions were not met.
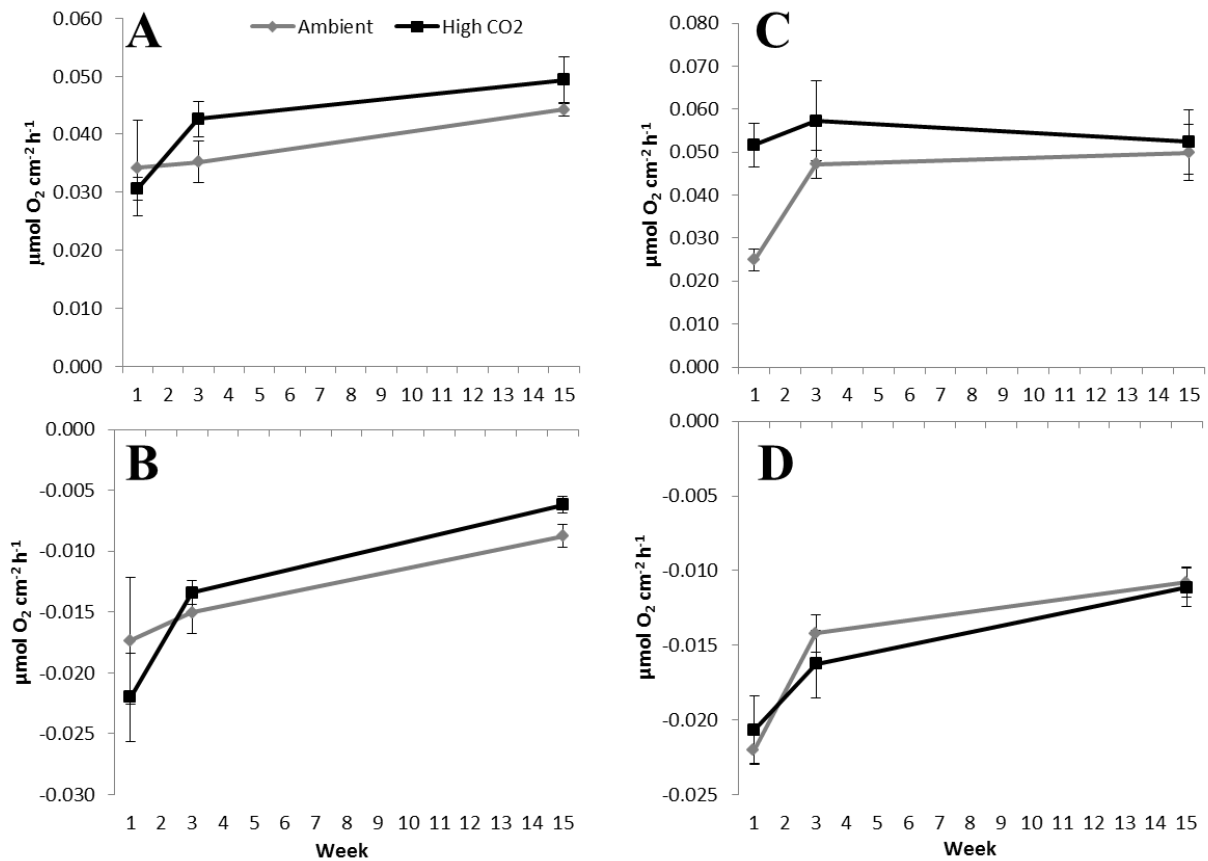
3.3.4 Alkalinity Anomaly

An independent samples t-test was performed to compare D. *stokesi* and *M. cavernosa* fragments' mean light and dark calcification rates (µmol $CaCO_3$ cm^{-2} h^{-1}) in ambient and high CO_2 conditions after fifteen weeks exposure. There were no significant differences in light calcification rates between treatment conditions for both of the species (t-test, $p>0.05$). Results from the independent samples t-tests indicated, however, that there were significant differences in dark calcification rates for *Montastraea cavernosa* only (Fig. 3.5). *Montastraea cavernosa* fragments grown in ambient seawater

(M = -0.118, SD = 0.15, n = 8) calcified significantly less after one hour in the dark than those in high CO_2 (M = 0.061, SD = 0.10, n = 5), t(11) = 2.335, p = 0.0395, while *Dichocoenia stokesi* fragments were not significantly different between treatments (t-test, p>0.05).

A two-way repeated measures ANOVA was used to analyze data for both light and dark calcification over three different time points for each species. There were no significant differences between the means of the treatment conditions, time point sampled, or the interaction of both. Both M. cavernosa and D. stokesi did not differ in their response overtime for light and dark calcification rates as determined through alkalinity anomaly under ambient and high CO_2 conditions.
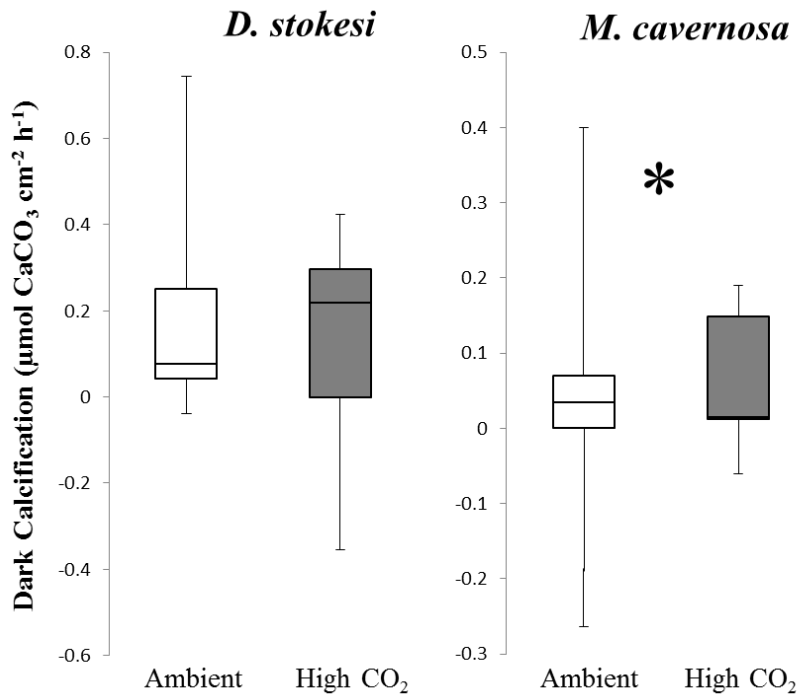
Figure 3.5: Average (mean ± SEM) of dark calcification (µmol $CaCO_3$ cm^{-2} h^{-1}) for *D. stokesi* and *M. cavernosa* in ambient (n=4,8) and high CO_2 (n=7,5) conditions for fifteen weeks. Asterisks represent significant differences (p < 0.05) between treatments determined using independent-samples t-test.

3.4   Discussion

Both *Dichocoenia stokesi* and *Montastraea cavernosa* exhibited a significant reduction in skeletal deposition rates after fifteen weeks exposure to high CO_2 conditions. This trend followed in newly deposited crystal length, where there was a significant reduction in crystal extension under the simulation of future oceans. No significant differences were seen in photosynthesis or respiration rates between treatment conditions; however, respiration rates for *M. cavernosa* displayed a significant reduction over time. These results suggest that the addition of CO_2 may cause a shift in the overall energy budgets causing a modification of skeletal aragonite crystal structures, rather than inhibiting skeletal crystal formation. Consequential to this energy shift, *Dichocoenia stokesi* and *Montastraea cavernosa* belong category group of scleractinian corals that exhibit a high sensitivity to ocean acidification (Ries 2011), and existing colonies will likely experience reduced growth rates or a decrease in the density of skeletal material in the face of ocean acidification.

3.4.1   Net Calcification

Recently developed models have identified two distinct classes of organisms exhibiting a low or high sensitivity to ocean acidification (Ries 2011; McCulloch et al. 2012). Measurements of growth rate paired with crystal structure data show that *D. stokesi* and *M. cavernosa* are at a high risk to experience growth impairments in ocean acidification conditions (Ries 2011; McCulloch et al. 2012). The crystal structure implies, along with reduced growth rates, that there may be a shift in the density and structural integrity of theses corals (Drenkard et al. 2013). Despite negative growth rates for *M. cavernosa* and *D. stokesi* in the high CO_2 treatment, both species were actively calcifying

under high CO_2 conditions as evidenced by the movement of organic matrix into the subcalicoblastic space through transmission electron micrographs (Fig. 5.2, appendix). Other studies have found skeletal integrity impairments under OA conditions for Caribbean species, which may further reduce the resilience of the already degraded population (Enochs et al. 2014; Holcomb et al. 2014; Tambutté et al. 2015). This sensitivity may be attributed to an inability to up-regulate pH of the subcalicoblastic fluid, removing fewer protons from the calcifying fluid under acidified conditions than under control conditions (Ries 2011). For restoration purposes, determining which species and genotypes are most resistant to climate change factors will be essential.

While both *M. cavernosa* and *D. stokesi* had a negative net calcification from buoyant weight measurements after fifteen weeks in high CO_2 conditions (-0.553 ± 0.25 and -0.532 ± 0.06 mg $CaCO_3$ cm^{-2} d^{-1} respectively), neither exhibited significant differences via alkalinity anomaly between the ambient and low pH seawater for light calcification. In addition, *M. cavernosa* experienced an increase in dark calcification in the high carbon dioxide treatment. Schoepf et al. (2013) also reported insignificant results for net calcification between treatment conditions across a wide range of pCO$_2$ values and coral species. The discrepancy with the buoyant weight data (e.g. loss of mass in ambient conditions for *M. cavernosa*) may relate to the surface area of the calcified skeletal structure that is exposed to seawater conditions. Even though the corals were successfully calcifying, as evidenced by data produced using the alkalinity anomaly technique and TEM images (Fig. 5.2, appendix), a loss of mass would occur if there was net dissolution taking place away from the active calcification sites over the entire diurnal period. Dissolution could be hidden from alkalinity anomaly data as the sampling period was only for one hour in a continuous process. Internal skeletal bioeroders were present

in *M. cavernosa*; bioeroders secrete an acidic compound to help create space in the CaCO$_3$ skeleton (Hutchings 1986). Their presence in ambient conditions contributes to the dissolution of skeletal material, but reduced pH in the water column due to ocean acidification may reduce the energy expense on these endolithic organisms and lead to even higher rates of erosion (Silbiger and Donahue 2015).

3.4.2   Physiology

The organisms that will be most susceptible under conditions of ocean acidification are those characterized by low basal metabolic rates, limited or no circulatory systems, and that precipitate a calcium carbonate skeleton proportionally larger than the organic component (Knoll et al. 2007). Stony corals, the framework builders of coral reefs globally, are a dominant group included in this description. The coral holobiont encompasses multiple organisms beyond the coral itself including bacteria and virus in the external mucus, tissue, and skeleton, zooxanthellae, endolithic algae, and bioeroders. All of these components interact; exchanging energy and nutrient-rich compounds. For this reason it is necessary to consider the role of energy acquisition through photosynthesis when looking at the coral hosts' physiological calcification mechanism. The relationship between photosynthesis and calcification in benthic calcifiers is poorly understood (Kleypas et al. 2006). Calcification rates can be enhanced by photosynthesis (Gattuso et al. 1999), but the stimulating mechanism remains poorly known (Cohen and McConnaughey 2003). Many studies have reported net photosynthetic rates of corals displaying either no response to increased pCO$_2$ or a slight increase (Langdon and Atkinson 2005; Schneider and Erez 2006; Anthony et al. 2008; Lürig and Kunzmann 2015). In this study, *D. stokesi* did not experience any significant change in photosynthetic output over time for fragments grown in high CO$_2$ conditions.

However, *M. cavernosa* fragments on average produced more oxygen in the high CO_2 treatment, regardless of the time sampled. These results indicate that increased carbon dioxide concentrations may have a positive impact on zooxanthellate productivity, but this is a coral species specific response and may be related to the *Symbiodium* clade present. *Symbiodinium* species are host specific; a single symbiont population was found in 92% of coral hosts in the Bahamas (LaJeunesse 2002). *Montastraea cavernosa* colonies collected from 2.5m were found to have only one type of symbiont of the C3e clade, while *D. stokesi* from the same location had only B1 *Symbiodinium* (LaJeunesse 2002). These genetic differences in zooxanthellae would explain the conflicting photosynthesis response for each of these species. Because growth deficiencies were experienced under OA conditions, additional energy supplied for photosynthesis by *M. cavernosa* symbionts did not mask the inefficiencies for pH regulation in the subcalicoblastic fluid.

Respiration values are typically stable under ocean acidification conditions (Leclercq et al. 2002; Anthony et al. 2008), consistent with what was experienced during this experiment. There was no significant effect of OA on respiration between treatments for each species after fifteen weeks of exposure. However, there was a clear and significant decrease in *M. cavernosa* respiration rates over time in either treatment. Given the similarity of these relationships, it is clear that a factor other than pCO_2 is influencing respiration rates, such as reduced stress over time due to acclimation to new seawater. These results indicate that, while carbon dioxide concentrations do not have an impact on oxygen consumption through respiration, these species are both acclimating over time to seawater conditions outside their normal conditions. This information may indicate ability for these species to adjust their energy budgets overtime to a more acidic ocean.

2.4.3   Electron Microscopy

Both *Dichocoenia stokesi* and *Montastraea cavernosa* experienced similar responses to ocean acidification with respect to nucleation of new skeletal crystals as measured by examining individual crystal lengths. They experienced no significant changes in length from week one to week fifteen of the experiment, regardless of treatment, and displayed a significant reduction in length from the control to the high CO_2 seawater. It appears that the impacts to crystal length are immediate and do not acclimate over time. As soon as the corals were exposed to the high CO_2 the change in the carbonate chemistry of the seawater led to a decrease in the extension of recently nucleated crystals. This may indicate that OA leads to a down-regulation of carbonic anhydrases, leading to a poor acid base regulation system. Carbonic anhydrases (CA) are enzymes that are responsible for the interconversion of carbon dioxide and bicarbonate. To this effect, the precipitation of calcium carbonate is promoted in the presence of CA (Rahman and Oomori 2010), which are strongly linked to pH regulation (Moya et al. 2012). Moya et al. (2012) found that OA lead to decreased expression of many CA's for *Acropora millepora*; furthermore 53% of this class of molecules responded to elevated CO_2.

Where skeletal material was present, all transmission electron micrographs illustrated the movement of organic matrix vacuoles to the subcalicoblastic space to initiate the nucleation of new skeletal material (Fig. 5.2, appendix). Corals have been documented producing new skeleton under pH levels as low as pH_T 7.17 (Holcomb et al. 2014). This same study found, however, that lateral growth rates (measured as changes in skeletal area) declined progressively with decreasing seawater pH, and growth was significantly reduced at pH_T 7.16 relative to ambient conditions (Holcomb et al. 2014).

The results of Holcomb et al. (2014) and this study suggest that crystal structure undergoes a species specific change in order to meet the energy demands of the organism (Fig. 3.2c).

Enhanced extracellular organic matrix gene expression was documented for *Acropora millepora* under high CO_2 (1000 ppm) conditions (Moya et al. 2012). Genetically distinct individuals responded differently toward the number and location of skeletal organic matrix genes they up-regulated or down-regulated, emphasizing the complexity of the dependence of microcalcification on the organic matrix. This altered expression and overall disturbance of the skeletal organic matrix could explain the changes in size, shape, and orientation of the aragonite crystals observed in this experiment as well as others (Cohen et al. 2009; Cohen and Holcomb 2009; Moya et al. 2012; Drenkard et al. 2013; Venn et al. 2013; Tambutté et al. 2015).

A recurring message in current ocean acidification research is that reduced calcium carbonate skeletal density is likely to be experienced by the end of the century. Enochs et al. (2014) found that high CO_2 levels (820-920 μatm) did not have an effect on skeletal extension but depressed the density of the skeletal crystals deposited. This was inferred as elevated pCO$_2$ did not affect linear extension, surface area, or volume of *Acropora cervicornis,* but significant differences were found in buoyant weight measurements between the treatments. The results of this study show that calcification of the Caribbean reef building species *D. stokesi* and *M. cavernosa* is negatively impacted under high pCO$_2$ conditions that are predicted to occur by the end of the century, and, with a shift in skeletal crystal structure, this may lead to reductions in skeletal density.

3.4.4   Conclusions

While it is unclear if *M. cavernosa* and *D. stokesi* are able to acclimate to persistent under exposure to high pCO$_2$ conditions, trends over time imply that fifteen weeks may not have been enough for these corals to acclimate to the shift in the carbonate system. In being transported and placed in a new seawater system, these corals experienced a change in water temperature, dissolved organics, nutrient levels, as well as light levels. Data from this experiment suggests that *M. cavernosa* may be better suited to physiologically acclimate to a more acidic ocean compared to *D. stokesi*. *Montastraea cavernosa* displayed a reduction in respiration rates, and a linear increase in photosynthetic activity, net calcification, and light calcification during the three sampling periods for both treatment conditions. *Dichocoenia stokesi*, however, experienced linear decreases in both net calcification and light calcification. To test the hypothesis that *M. cavernosa* is better suited to acclimate to high CO$_2$ conditions, studies should monitor individual genotypes. The time it takes for this species to acclimate may not be feasible for laboratory experimentation.

The response of coral calcification to ocean acidification is ultimately dictated by the limits of coral physiology to acclimate or adapt to a more acidic ocean rather than just kinetics alone (McCulloch et al. 2012). It is crucial to continue understanding how OA will influence all coral reef organisms as their interactions create this ecosystem. Found here is that elevated pCO$_2$ significantly affected net calcification, while having no negative effect on physiology parameters. Other members of the coral holobiont, such as endolithic algae and bacterial communities, may mask a physiological response of the coral animal to high CO$_2$ conditions. A distinct qualitative difference in the skeletal crystals produced in ambient versus high CO$_2$ seawater, a relationship that varied

between species was also found. The results suggest that as $p\mathrm{CO}_2$ levels increase over time, coral growth will be influenced by altering skeletal density of recent and previously deposited skeletal crystals. This could have broad implications for the structural integrity and longevity of Caribbean coral colonies that must withstand natural physical and biological disturbances under increased OA scenarios.

Through lowered skeletal density, ocean acidification could be linked to the decline of coral reefs with an associated loss in biodiversity, productivity, and revenue. Given the strong interactions that work together in the coral holobiont to support the biological production of calcium carbonate, the coral animal cannot be evaluated in isolation. Instead, other impacts such as photophysiology response and energy balance must be evaluated in synergy (Anthony et al. 2008). As scientists, it is our intention to develop and demonstrate innovative tools and technologies for providing information and capacity to adequately prepare for climate-induced changes in the marine environment. A major goal this research is to gain a better understanding of the influence of a more acidic ocean and to establish ways for climate scientists, impact assessment modelers, air and water quality managers, and other stakeholders to co-produce information necessary to form sound policy in relation to ocean acidification and its impact on marine water quality under a changing climate. This discussion is necessary to examine the mechanism behind species specific response to a less alkaline world.

Chapter 4

4   Discussion

Of the major environmental factors associated with the global distribution of coral reefs, most will be disrupted under conditions of global climate change (Kleypas et al. 2006). To date, there have been many studies evaluating the responses of adult corals (Anthony et al. 2008; Marubini et al. 2008; Holcomb et al. 2012; Moya et al. 2012; Schoefp et al. 2013; Enochs et al. 2014; Holcomb et al. 2014), juveniles (de Putron et al. 2011; Drenkard et al. 2013) or larval physiology and settlement (Albright et al. 2008; Cohen et al. 2009; Albright et al. 2010; Albright and Langdon 2011; Cumbo et al. 2013) under ocean acidification conditions. However, there still remains a gap in knowledge as many projects have included just a handful of species. It is crucial to continue understanding how OA will influence all coral reef organisms as their interactions create this ecosystem. Here I found that elevated pCO$_2$ significantly affected net calcification in some, but not all tested species, while having no effect on physiology parameters or calcification via alkalinity anomaly. I also found a distinct quantitative difference in the skeletal crystals produced in ambient versus high CO$_2$ seawater. Crystal structure for *O. faveolata* under high CO$_2$ most closely resembled *D. stokesi* fragments grown in the control treatment. This suggests that CO$_2$ levels influence growth by altering skeletal density of recent and previously deposited skeletal crystals. This could have broad implications for the structural integrity and longevity of Caribbean coral colonies that must withstand natural physical and biological disturbances under increased OA scenarios. The economic benefits of coral reefs come from recreation, tourism, fisheries, pharmaceuticals, and coastal protection. All of these factors, including the invaluable biodiversity, are a result of the three dimensional structure of a reef created by

hermatypic corals. The production of a structurally sound coral skeleton is therefore required to create and maintain these valuable ecosystems.

Recent evidence suggests that OA leads to an increase in corallite calyx (the perimeter around a given corallite), decreasing the total number of corallites in a given area of living tissue (Tambutté et al. 2015). This change decreases the skeletal density and increases the porosity of a given sample. From this information, it may be implied that species exhibiting smaller polyps initially (such as *O. faveolata*) and those with greater skeletal densities (e.g. *D. stokesi*) may not suffer as much if the corallite calyx size increased.

The goal of this project was to answer two specific questions to further our understanding of coral reef dynamics in a more acidic ocean:

1. **Will decreased pH affect fine scale calcification in *O. faveolata* recruits and adults?**

2. **Are *M. cavernosa* and *D. stokesi* able to acclimate under persistent exposure to high pCO$_2$ conditions*?***

4.1   Net Calcification

Both buoyant weight and alkalinity anomaly methods yield net calcification values; i.e., gross calcification minus dissolution. The buoyant weight and alkalinity anomaly methods have the advantage of being nondestructive (Kleypas et al. 2006), but do not always agree with each other (E. Hall, pers. comm.). Because the corals used in this experiment are imperforate, there is only a small portion of the mass that represents the tissue components, and thus, greater than 99% of the mass is skeletal material (Davies 1989). Net calcification has typically been shown to decline with climate stressors such

as ocean acidification. The magnitude of decline differs between species and is highly variable (Anthony et al. 2008; Ries et al. 2009, de Putron et al. 2011; Pandolfi et al. 2011; Silbiger and Donahue 2015). While both *M. cavernosa* and *D. stokesi* had a negative net calcification from buoyant weight measurements after fifteen weeks in high CO_2 conditions (-0.553 ± 0.25 and -0.532 ± 0.06 mg $CaCO_3$ cm^{-2} d^{-1} respectively), neither exhibited significant values between the ambient and low pH seawater using the alkalinity anomaly technique.

The discrepancy in the buoyant weight data (e.g. loss in mass in ambient conditions for *M. cavernosa*) may relate to the surface area of the calcified skeletal structure that is exposed to seawater conditions. Even though the corals were successfully calcifying, as evidenced by data produced using the alkalinity anomaly technique and TEM images (Fig. 5.2, appendix), a loss of mass would occur if there was net dissolution taking place away from the active calcification sites over the entire diurnal period. Dissolution could be hidden from alkalinity anomaly data as the sampling period was only for one hour in a continuous process. The discrepancy with the buoyant weight data (e.g. loss of mass in ambient conditions for *M. cavernosa*) may also relate to the surface area of the calcified skeletal structure that is exposed to seawater conditions. *Montastraea cavernosa* experienced a trifecta of circumstances that explain a negative net calcification rate even in ambient conditions: low light and dark calcification rates, high skeletal exposure, and the presence of natural bioeroders in the internal skeleton. Bioeroders secrete an acidic compound to help create space in the $CaCO_3$ skeleton (Hutchings 1986). Their presence in ambient conditions contributes to the dissolution of skeletal material, but reduced pH in the water column due to ocean acidification may reduce the energy expense on these endolithic organisms and lead to even higher rates of

erosion (Silbiger and Donahue 2015). Previous studies have also presented insignificant results for net calcification between treatment conditions across a wide range of pCO$_2$ values and coral species (Schoepf et al. 2013).

In this experiment, *O. faveolata* had no significant change in growth under both buoyant weight measurements and displayed elongated crystal structures compared to the control (Fig. 2.1). This unusual response of calcification in a low pH, and therefore low Ω_{arag}, environment may be explained by the genetic variation leading to a range of species sensitivity to OA. Some corals maintain ambient calcification rates over large ranges of Ω_{arag} conditions, possibly explained as evolution selecting for species/genotypes that are highly efficient calcifiers or those that direct a higher proportion of their energy budget to calcification (Pandolfi et al. 2011). This lowered sensitivity compared to the other species may be explained in the pH up-regulation system of the calcifying fluid. Through Ca-ATPase antiporters in the calicodermis, coral remove two protons from the subcalicoblastic fluid in exchange for a calcium ion (Al-Horani et al. 2003; Holcomb et al. 2009). This process is energy expensive, but in the presence of excess ATP, corals can establish high internal aragonite saturation states despite sharp changes in pH. Energy expenditure on calcification is generally around one-third of that produced from photosynthesis of *Symbiodinium sp.* (McCulloch et al. 2012). Although the results support the idea that corals may be able to up-regulate pH at the site of calcification resulting in nucleation of new skeletal crystals, the crystal structure implies that there may be a shift in the structural density of the coral (McCulloch et al. 2012). Other studies have found skeletal integrity impairments under OA conditions for Caribbean species, which may further reduce the resilience of the already degraded population (McCulloch et al. 2012; Enochs et al. 2014; Holcomb et al. 2014; Tambutté et

al. 2015). Additionally, overall health of coral reef systems may shift drastically with the compounding effects of increasing thermal stress from global warming and local environmental impacts (Pandolfi et al. 2011; McCulloch et al. 2012; Cumbo et al. 2013; Schoepf et al. 2013). For restoration purposes, determining which species and genotypes are most resistant to climate change factors will be essential.

Despite the significant differences determined through buoyant weight data, there were no significant results for light calcification and only inconclusive significance for dark calcification (i.e. dark calcification was higher in the CO_2 treatment for *M. cavernosa* where growth rate had significantly decreased and vice versa for *O. faveolata*) using the alkalinity anomaly technique. This inconsistency in calcification data can be explained. I measured carbonate uptake over a two hour period; this period of time is likely too short to cover the range of internal chemical conditions that the corals experience daily. Additionally, by recording buoyant weights at the beginning and throughout the experiment, this data can take into account full diurnal cycles and any mechanical erosion that takes place slowly in the tanks. A species specific trend across time emerges when all the data is combined. Day time calcification decreased over time for *D. stokesi* in both treatment conditions (Fig. 3.6a), which corresponds well to buoyant weight data. This negative trend indicates that *D. stokesi* has a low acclimation potential, though large standard error bars may point to genotypic variance. *Montastraea cavernosa*, despite having a negative net calcification over the experimental period, had a linear increase in light calcification rates for both the ambient and high CO_2 treatment. Again, this data follows the patterns of the buoyant weight results, supporting the idea that *M. cavernosa* has high acclimation potential for a more acidic ocean, given enough time. *Montastraea cavernosa* and *O. faveolata* displayed higher light calcification rates in

ambient seawater across all time periods, contrary to photosynthesis results, indicating that the relationship between calcification and *Symbiodinium* activity may be uncoupled.

4.2   Physiology

The organisms that will be most vulnerable under conditions of ocean acidification are those characterized by low basal metabolic rates, limited or no circulatory system, and that precipitate a calcium carbonate skeleton proportionally larger than the organic component (Knoll et al. 2007). Stony corals, the framework builders of coral reefs globally, are a dominant group included in this description. However, there are multiple partners that make up the holobiont. All of these components interdepend at the most basic metabolic level (Horwitz et al. 2015). *Symbiodinium*, the symbiotic dinoflagellate present in zooxanthellate corals, such as the ones used in this experiment, utilize bicarbonate (HCO_3^-) instead of $CO_{2(aq)}$, as the primary source for photosynthesis (Kleypas et al. 2006; Brading et al. 2013). Bicarbonate concentrations will increase about 14% under doubled CO_2 conditions (Kleypas et al. 2006). Extrinsic sources of carbon for the host include zooplankton and particulate organic carbon (POC). The interaction of these organisms includes exchanging energy and nutrient-rich compounds, hence it is imperative to consider the role of *Symbiodinium* energy acquisition through photosynthesis when looking at the coral host's physiological process of calcification. The relationship between photosynthesis and calcification in benthic calcifiers remains poorly understood (Kleypas et al. 2006). Previous research has documented that calcification rates in corals can be enhanced by photosynthesis (Gattuso et al. 1999), but the stimulating mechanism remains poorly known (Cohen and McConnaughey 2003). Many studies have reported net photosynthetic rates of corals displaying either no response to increased $p\mathrm{CO}_2$ or a slight increase (Langdon and Atkinson 2005; Schneider

and Erez 2006; Anthony et al. 2008; Lürig and Kunzmann 2015). In this study, though some significantly higher photosynthetic rates were seen at increased CO_2 concentrations *for M. cavernosa* (Fig. 3.4c), the trend did not lead to an increased accumulation of skeletal material. *Symbiodinium* species are host specific; a single symbiont population was found in 92% of coral hosts in the Bahamas (LaJeunesse 2002). *Montastraea cavernosa* colonies collected from 2.5m were found to have only one type of symbiont of the C3e clade, while *D. stokesi* from the same location had only B1 *Symbiodinium*, and *O. faveolata* was found to only host clade C7 (LaJeunesse 2002). These genetic differences in zooxanthellae would explain the conflicting photosynthesis response for each of these species. Because growth deficiencies were experienced under OA conditions, additional energy supplied for photosynthesis by *M. cavernosa* symbionts did not mask the inefficiencies for pH regulation in the subcalicoblastic fluid. For the species that experienced a non-significant photosynthetic response to increase pCO_2, it's plausible that the photosynthetic benefit of an increased CO_2 supply may be overridden by the disruption of photophysiological processes (Anthony et al. 2008). Though higher concentrations of bicarbonate are present under OA conditions, low pH may interfere with the pathway for CO_2 accumulation thereby directly affecting the ability of the individual symbionts to fix carbon (Anthony et al. 2008). There is a gap in research on the molecular and biochemical pathways of the photosynthesis-calcification relationship; understanding this relationship is required before the effect of environmental changes on coral physiology can be deciphered.

High respiration rates can be an indication of high metabolic activity and stress (Lürig and Kunzmann 2015) or evidence that the coral animal is not receiving enough energy from *Symbiodinium* photosynthesis. *Montastraea cavernosa* had a reduced

respiration rate over time, regardless of treatment. During an eight week study, Anthony et al. (2008) found significant depressions in daily productivity (hourly rate of photosynthesis – respiration integrated over the day) for *Acropora intermedia* and *Porites lobata* at pH conditions of 7.70-7.60. In some cases productivity dropped close to zero and it was determined that the simulated ocean acidification conditions affected net photosynthetic rates only, whereas rates of dark respiration were relatively stable. Stable respiration rates were also present for Leclercq et al. (2002). While this study suggests that experimental duration, specifically the length of acclimation, can influence the organisms response to OA (i.e., respiration and photosynthesis rates of *D. stokesi* and *M. cavernosa* changed linearly over the experimental period indicating they were not completed acclimated, see Fig. 3.4), it is likely that biological aspects have a stronger influence on the sensitivity of coral calcification to OA than differences in methods (Scheopf et al. 2013). There is a clear trend toward a reduction in respiration over time for D. *stokesi* and *M. cavernosa*, observable both treatment conditions. This may indicate that the corals become less stressed as they continuously acclimating to new seawater environments, regardless of the carbonate system composition.

4.3   Electron Microscopy

Where skeletal material was present, all transmission electron micrographs confirmed the movement of organic matrix vacuoles to the subcalicoblastic space to initiate the nucleation of new skeletal material (Fig. 5.2, appendix). Corals have been documented producing new skeleton under pH levels as low as pH_T 7.17 (Holcomb et al. 2014). This same study found, however, that lateral growth rates (measured as changes in skeletal area) declined progressively with decreasing seawater pH, and growth was significantly reduced at pH_T 7.16 relative to ambient conditions (Holcomb et al. 2014).

Enhanced extracellular organic matrix gene expression was documented for *Acropora millepora* under high CO_2 (1000 ppm) conditions (Moya et al. 2012). Individuals responded differently toward the number and location of skeletal organic matrix genes they up-regulated or down-regulated, emphasizing the complexity of the dependence of microcalcification on the organic matrix. This altered expression and overall variability in production of the skeletal organic matrix could explain the changes in size, shape, and orientation of the aragonite crystals observed in this experiment as well as others (Cohen et al. 2009; Cohen and Holcomb 2009; Moya et al. 2012).

For many organisms, the function of $CaCO_3$ varies with life cycle stage (e.g., planktonic stages, recruitment), but almost all studies of CO_2 effects on calcification have focused on adults (Kleypas et al. 2006). Understanding the effects of OA on calcification for newly settled recruits as well as understanding how adults of the same species responds helps us understand the true impact of OA across an individual. Slowed juvenile growth would mean more time spend in the juvenile stage therefore lengthening the period where the corals are not sexually reproductive. In combination with adult loss, population structures would shift toward smaller class sizes, decreasing effective population sizes and population fecundity (Albright and Langdon 2011). The results from this experiment show a similar response in skeletal structure for adult and newly recruited *O. faveolata* in each of the treatment conditions. In high CO_2 (>1450 ppm) treatment seawater, this species displayed longer crystal growth (Fig. 2.1), indicating the ability to nucleate and grow crystals more efficiently than corals grown in the ambient condition (Cohen and Holcomb 2009). This appears to be a species specific response and was consistent between different genets. Growth of juvenile spat, from the brooding *Favia fragum*, was unaffected by OA induced by significantly elevated levels of CO_2 (Drenkard

et al. 2013). However, Cohen et al. (2009) found that the shape of the basal plate of *F. fragum* spat became distorted as saturation state decreased. The irregular basal plate, paired with an incomplete rim, can prevent an effective seal around the calcifying region. Exposure to external seawater in the calcifying fluid will exacerbate the challenges for calcification the organism is already experiencing in a low pH environment (Cohen et al. 2009). Qualitatively, I did not see a difference in rim development between treatment conditions and across time (Fig. 5.1, appendix). Venn et al. (2013) found that new crystal growth for *Stylophora pistillata*, as measured by changes in cross-sectional area, for corals maintained at pH 8, pH 7.8, and pH 7.4 showed no significant difference. These results, along with our data, imply that there is a physiological resilience across many distinctly different species when considering active calcification.

A recurring message in current ocean acidification research is that reduced calcium carbonate skeletal density is likely to be experienced by the end of the century. Enochs et al. (2014) found that high CO_2 levels (820-920 μatm) did not have an effect on skeletal extension but depressed the density of the skeletal crystals deposited. This was inferred as elevated $p\text{CO}_2$ did not affect linear extension, surface area, or volume of *Acropora cervicornis* but significant differences were found in buoyant weight measurements between the treatments. The results of this study and that of Enochs et al. (2014) show that calcification of the Caribbean reef building species *D. stokesi* and *M. cavernosa* is negatively impacted under high $p\text{CO}_2$ conditions that are predicted to occur by the end of the century through reductions in skeletal density. There does not appear to be a trend over time in crystal length, though this may be influenced by the difficulty in imaging identical locations between different species and across time.

The mechanism of coral calcification is not fully understood (Cohen and McConnaughey 2003; Cohen and Holcomb 2009; Allemand et al. 2011; Ries 2011), largely in part to the small size and location of the subcaliceblastic space. Two well explored models are the physicochemical model, which asserts that the calcifying fluid of corals is initially similar to that of their external seawater and skeletal accretion occurs when arag is increased via Ca-ATPase-driven exchange of Ca^{2+} and H^+ ions across the coral tissue (e.g. Al-Horani et al. 2003, Cohen and McConnaughey 2003, Cohen and Holcomb 2009; Allemand et al. 2011), and the biological model that describes calcification as a function of calicoblastic cell and organic matrix activity (Houlbreque et al. 2009) completely independent of the chemical changes in the coral's external seawater (Meibom et al. 2008). This study, along with recent work on gene expression (Moya et al. 2012), suggests that a combination of these models drives skeletal crystal formation. Enhanced extracellular organic matrix gene expression was documented for *Acropora millepora* under high CO_2 (1000 ppm) conditions (Moya et al. 2012), that is, the chemistry of the seawater (physicochemical model) lead to a shift in the expression of organic matrix genes (biological model), likely resulting in growth changes. The present study shows that altered seawater chemistry, achieved via carbon dioxide elevation, can cause a shift in the morphology of crystal structure, supporting the physicochemical model. However, calcification was occurring at low pH values, evidenced by the presence of organic matrix vacuoles passing from the calicoblastic endoderm into the calcifying fluid (Fig. 5.2, appendix). The organic matrix supports the nucleation of calcium carbonate in conditions that may not be thermodynamically favorable (Houlbreque et al. 2009), indicating that the biological model is equally valid. Ultimately, the level of dependence of microcalcification on the organic matrix is still unknown.

4.4   Conclusions and Future Research

In addressing the question: "Will changes in pH affect fine scale calcification during the earliest life history stages and in adults of *O. faveolata*," the answer is yes. Though *O. faveolata* was recently added to the IUCN threatened species list, this species appears to be well suited for a more acidic environment. This observation is based on the results that *O. faveolata* grew significantly better than *M. cavernosa* and *D. stokesi* under high CO_2 conditions. Additionally, the crystal structure of recently nucleated skeletal material was statistically longer in the low pH treatment, an indication of healthier growth (Cohen and Holcomb 2009). This crystal length trend existed across generational boundaries as the recently settled spat also displayed longer crystals in the high CO_2 treatment. Ideally, it would be best to rear adults in high CO_2 seawater through the process of sexual reproduction and to settle out individuals with known parents to evaluate the adaptation potential for this species. However, rearing spat is difficult without the obstacle of reduced pH and few survive to adult hood (N. Fogarty pers. comm.). In being able to sustain and even enhance calcification under high CO_2 conditions, *O. faveolata* could be diverting energy away from other critical life processes such as tissue growth or reproduction. This relatively short (12 week) experiment cannot quantify changes in other physiology aspects; understanding the long term effects of ocean acidification would require a longer experimental period.

While it is unclear if *M. cavernosa* and *D. stokesi* are able to acclimate to persistent exposure to high pCO_2 conditions, trends over time imply that fifteen weeks may not have been long enough for these corals to adjust to the new seawater (Sarasota Bay vs Atlantic), let alone the change in the carbonate system. Data from this experiment supports the idea that *M. cavernosa* may be better suited to physiologically acclimate to a

more acidic ocean in comparison to *D. stokesi*. *M. cavernosa* displayed a reduction in respiration rates, a linear increase in photosynthetic activity, net calcification via buoyant weights, and light calcification during the three sampling periods for both treatment conditions. *Dichocoenia stokesi*, however, experienced linear decreases in both mass change and light calcification. To prove the hypothesis that *M. cavernosa* is better suited to acclimate to high CO_2 conditions, studies are needed to determine exactly what length of time is required to acclimate for individual genotypes of this species. The time it takes for this species to acclimate may be unfeasible for laboratory experimentation.

Through lowered skeletal density, ocean acidification could be linked to the decline of coral reefs leading to an associated loss in biodiversity, productivity, and revenue. Given the strong interactions that work together in the coral holobiont to support the biological production of calcium carbonate, the coral animal cannot be evaluated in isolation. Instead, other impacts such as photophysiology response and energy balance must be evaluated in synergy (Anthony et al. 2008). It is our intention as scientists to develop and demonstrate innovative tools and technologies for providing information and capacity to adequately prepare for climate-induced changes in the marine environment. A major goal this research is to gain a better understanding of the influence of a more acidic ocean and to establish ways for climate scientists, impact assessment modelers, air and water quality managers, and other stakeholders to co-produce information necessary to form sound policy in relation to ocean acidification and its impact on marine water quality under a changing climate. This discussion is necessary to examine the mechanism behind species specific response to a less alkaline world.
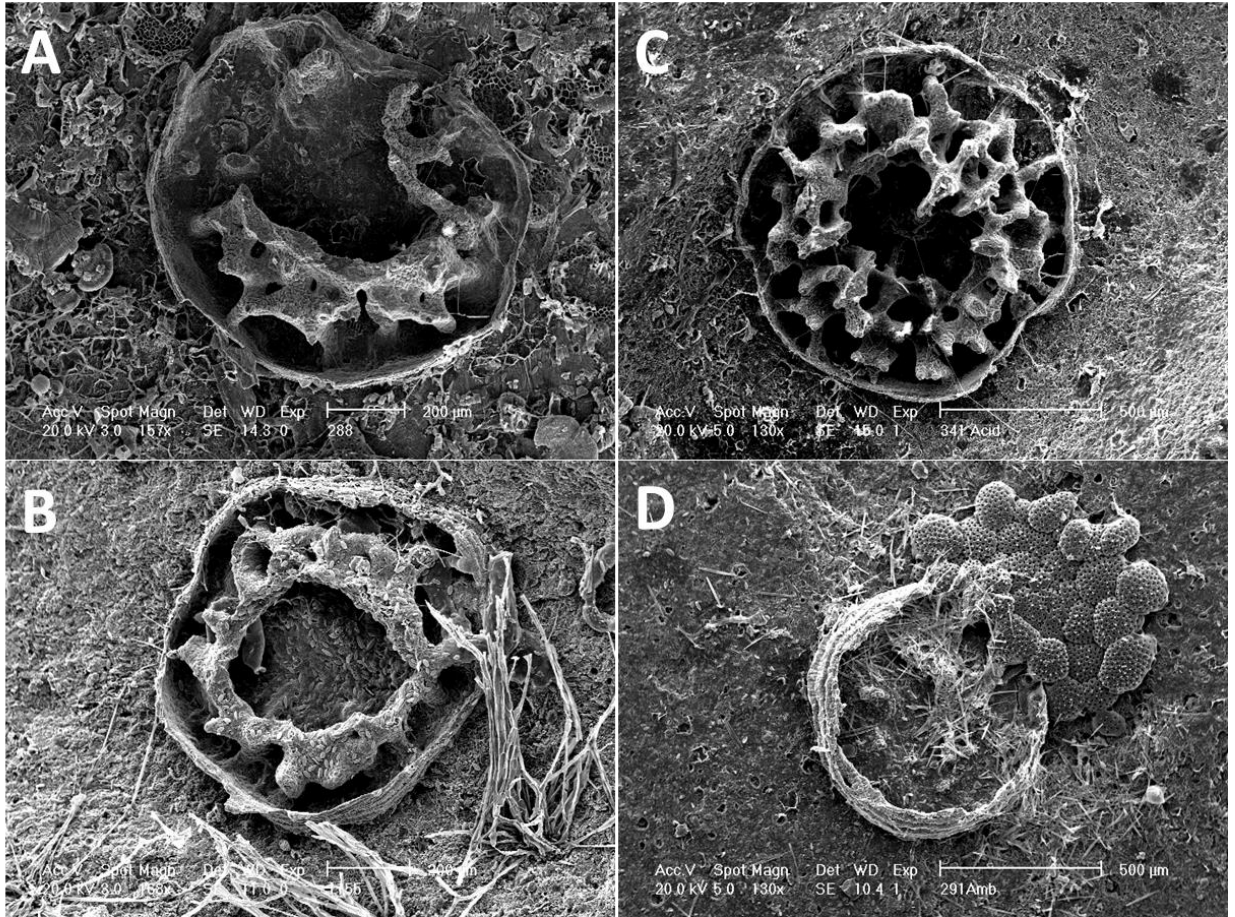
Figure 5.1: Scanning electron micrographs of juvenile *Orbicella faveolata* spat imaged after one (A,B) or two (C,D) weeks in high CO_2 (pH_{NBS} 7.71, A,C) and ambient (pH_{NBS} 8.14, B,D) conditions. Scale bars are 200 µm for A,B and 500µ m for C,D.
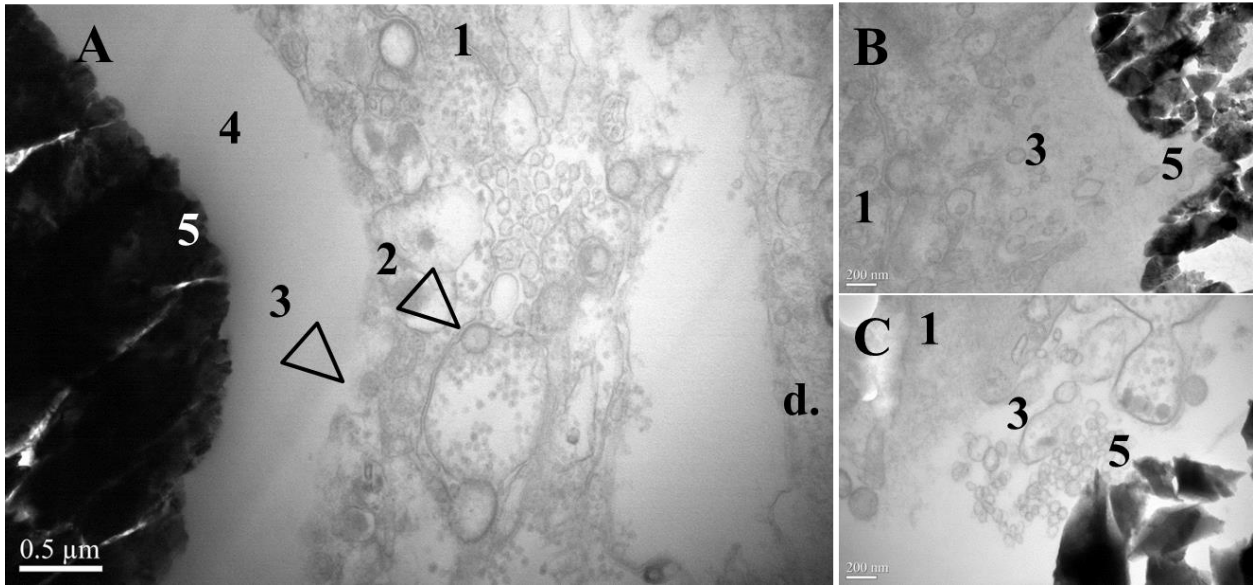
Figure 5.2: Transmission electron micrographs displaying the calcification interface in *D. stokesi*, week 3, high CO_2 (A), and *M. cavernosa*, weeks 1 and 3, high CO_2 (B and C respectively). The calicoderm (1) produces vacuole containing organic matrix (2), which are then exocytosed by the cells (3) into the subcalicoblastic fluid (4) where they serve as the nucleation sites for new skeletal crystals (5).

References

Aeby GS, Work TM, Runyon CM, Shore-Maggio A, Ushijima B, Videau P, Beurmann S, Callahan SM (2015) First record of black band disease in the Hawaiian archipelago: response, outbreak status, virulence, and a method of treatment. PLoS ONE 10(3): e0120853. doi:10.1371/journal.pone.0120853

Al-Horani FA, Al-Moghrabi SM, de Beer D (2003) The mechanism of calcification and its relation to photosynthesis and respiration in the scleractinian coral *Galaxea fascicularis*. Marine Biology 142:419-426. doi: 10.1007/s00227-002-0981-8.

Albright R, Langdon C (2011) Ocean acidification impacts multiple early life history processes of the Caribbean coral *Porites astreoides*. Global Change Biology 17(7):2478-2487. doi: 10.1111/j.1365-2486.2011.02404.x.

Albright R, Mason B, Langdon C (2008) Effect of aragonite saturation state on settlement and post-settlement growth of *Porites astreoides* larvae. Coral Reefs 27:485–490. doi:10.1007/s00338-008-0392-5

Albright R, Mason B, Miller M, Langdon C (2010) Ocean acidification compromises recruitment success of the threatened Caribbean coral Acropora palmata. PNAS 107(47):20400-20404.

Allemand D, Tambutté E, Zoccola D, Tambutté S (2001) Coral reefs: An ecosystem in transtion Vol. III. Dubinsky Z, Stambler N (eds) Springer:119-150.

Andersson AJ, Mackenzie FT, Bates NR (2008) Life of the margin: implications of ocean acidification on Mg-calcite, high latitude and cold-water marine calficiers. Marine Ecology Progress Series 373:265-272.

Andersson AJ, Kuffner IB, Mackenzie FT, Jokiel PL, Rodgers KS, Tan A (2009) Net loss of $CaCO_3$ from a subtropical calcifying community due to seawater acidification: mesocosm-scale experimental evidence. Biogeosciences 6:1811-1823.

Anthony KRN, Kline DI, Diaz-Pulido G, Dove S, Hoegh-Guldberg O (2008) Ocean acidification causes bleaching and productivity loss in coral reef builders. PNAS 105 (45):17442-17446. doi: 10.1073/pnas.0804478105.

Arenasa F, Vaz-Pintob F (2014) Marine Algae as Carbon Sinks and Allies to Combat Global Warming. Marine Algae: Biodiversity, Taxonomy, Environmental Assessment, and Biotechnology: 178.

Brading P, Warner ME, Smith DJ, Suggett DJ (2013) Contrasting modes of inorganic carbon acquisition amongst *Symbiodinium* (Dinophyceae) phylotypes. New Phytol. 200:432–442.

Brander L, van Beukering P (2013) The Total Economic Value of U.S. Coral Reefs: A Review of the Literature. NOAA Coral Reef Conservation Program. Silver Spring, MD: NOAA

Brewer PG (2009) A changing ocean seen with clarity. PNAS 106 (30):12213-12214.

Brewer PG, Barry, J (2008) The other CO_2 problem. Scientific American 18(4): 22-2.

Budd AF, Fukami H, Smith ND, Knowlton N (2012) Taxonomic classification of the reef coral family Mussidae (Cnidaria: Anthozoa: Scleractinia). Zoological Journal of the Linnean Society 166:465-529

Budd AF, Nunes FLD, Weil E, Pandolfi JM (2011) Polymorphism in a common Atlantic reef coral (*Montastraea cavernosa*) and its long-term evolutionary implications. Evolutionary Ecology 26(2):265-290.

Caldeira K, Wickett ME (2003) Anthropogenic carbon and ocean pH. Nature 425:365.

Cesar H, Burke L, Ret-Soede L (2003) The economics of worldwide coral reef

degradation. Cesar Environmental Economics Counsulting (CEEC); 3rd ed.

Inspiration Company, Arnhem, Netherlands.

Chiappone M, Sullivan KM (1996) Distribution, abundance and species composition of

juvenile scleractinian corals in the Florida reef tract. Bulletin of marine

science 58(2):555-569.

Cohen AL, Holcomb M (2009) Why corals care about ocean acidification: uncovering

the mechanism. Oceanography 22(4):118-127.

Cohen AL, McConnaughey TA (2003) Geochemical Perspectives on Coral

Mineralization. Reviews in Mineralogy and Geochemistry 54 (1):151-187. doi:

10.2113/0540151.

Cohen AL, McCorkle DC, de Putron S, Gaetani GA, Rose KA (2009) Morphological and

compositional changes in the skeletons of new coral recruits reared in acidified

seawater; insights into the biomineralization response to ocean acidification.

Geochemistry, Geophysics, Geosystems - G3 10 (7):Q07005. doi:

http://dx.doi.org/10.1029/2009GC002411.

Comeau S, Carpenter RC, Edmunds PJ (2012) Coral reef calcifiers buffer their response

to ocean acidification using both bicarbonate and carbonate. Proceedings of the

Royal Society B: Biological Sciences 280 (1753). doi: 10.1098/rspb.2012.2374.

Costanza R, d'Arge R, de Groot R, Farbar S, Grasso M, Hannon B, Limburg K, Naeem S,

O'Neill RV, Parnero J, Raskin JP, Sutton P, van den Belt M (1997) The value of

the world's ecosystem services. Nature 387:253-260.

Cumbo VR, Edmunds PJ, Wall CB, Fan T (2013) Brooded coral larvae differ in their response to high temperature and elevated pCO$_2$ depending on the day of released. Mar Biol 160:2903-2917.

Cury P, Shannon L, Shin YJ (2003) The functioning of marine ecosystems: a fisheries perspective. Responsible fisheries in the marine ecosystem: 103-123.

Davies PS (1989) Short-term growth measurements of corals using an accurate buoyant Iighing technique. Marine Biology 101:389-395.

de Putron SJ, McCorkle DC, Cohen AL, Dillon AB (2011) The impact of seawater saturation state and bicarbonate ion concentration on calcification by new recruits of two Atlantic corals. Coral Reefs 30:321-328.

Dickson AG (1990) Standard potential of the reaction: AgCl(s) + 1/2H$_2$(g) = Ag(s) + HCI(aq), and the standard acidity constant of the ion HSO$_4$ in synthetic sea water from 273.15 to 318.15 K. Journal of Chemical Thermodynamics 22:113-127.

Dickson AG, Millero F (1987) A comparison of the equilibrium-constants for the dissociation of carbonic-acid in seawater media. Deep Sea Res A: 1733-1743.

Dickson AG, Sabine CL, Christian JR (eds) (2007) Guide to Best Practices for Ocean CO$_2$ Measurements. In *PICES Special Publication 3*, Sidney, BC, Canada

Doney SC, Fabry VJ, Feely RA, Kleypas JA (2009) Ocean acidification: the other CO$_2$ problem. Marine Science; 1. doi:10.1146/annurev.marine.010908.163834.

Drenkard EJ, Cohen AL, McCorkle DC, de Putron SJ, Starczak VR, Zicht AE (2013) Calcification by juvenile corals under heterotrophy and elevated CO$_2$. Coral Reefs 32:727–735. doi:10.1007/s00338013-1021-5

Enochs IC, Manzello DP, Carlton R, Schopmeyer S, Hooidonk R, Lirman D (2014) Effects of light and elevated pCO$_2$ on the growth and photochemical efficiency of

Acropora cervicornis. Coral Reefs 33(2):477-485. doi:
http://dx.doi.org/10.1007/s00338-014-1132-7.

Fabricius K, Langdon C, Uthicke S, Humphrey C, Noonan S, De'ath G, Okazaki R,
Muehllehner N, Glas M, Lough J (2011) Losers and winers in coral reefs
acclimatized to elevated carbon dioxide concentrations. Nature Climate Change
1:165-169.

Feely RA, Doney SC, Cooley SR (2009) Present conditions and future changes in a high-
CO_2 world. Oceanography 22(4):36.

Findlay HS, Wood HL, Kendall MA, Spicer JI, Twitchett RJ, Widdicombe S (2009)
Calcification, a physiological process to be considered in the context of the whole
organism. Biogeosciences Discussions 6(1):2267-2284.

Gattuso J-P, Allemand D, Frankignoulle M (1999) Photosynthesis and calcification at
cellular, organismal and community levels in coral reefs: A review on interactions
and control by carbonate chemistry. Am. Zool. 39:160–183.

Gattuso J-P, Frankignoulle M, Bourge I, Romaine S (1998) Effect of calcium carbonate
saturation of seawater on coral calcification. Glob. Planet. Change 18:37-46.

Gattuso J-P, Hansson L (2011) *Ocean Acidification*. New York: Oxford University Press
Inc.

Gledhill D, Wanninkhof R, Millero F, Eakin M (2008) Ocean acidification of the Greater
Caribbean Region 1996–2006. J. Geophys. Res. 113

Glynn PW, Peters EC, Muscatine L (1985) Coral tissue microstructure and necrosis:
relation to catastrophic coral mortality in Panama. Dis Aquat Org, 1:29-37.

Goreau TF (1959) The ecology of Jamaican coral reefs. I. Species composition and
zonation. Ecology 40:67–90

Goreau TF, Wells JW (1967) The shallow-water Scleractinia of Jamaica: revised list of
species and their vertical distribution range. Bull Mar Sci 17:442–453.

Hoegh-Guldberg O, Mumby PJ, Hooten AJ, Steneck RS, Greenfield P, Gomez E, Harvell
CD, Sale PF, Edwards AJ, Caldeira K, Knowlton N, Eakin CM, Iglesias-Prieto R,
Muthiga N, Bradbury RH, Dubi A, Hatziolos ME (2007) Coral Reefs Under
Rapid Climate Change and Ocean Acidification. Science 318(5857):1737-1742.

Holcomb M, Cohen AL, McCorkle DC (2012) An investigation of the calcification
response of the scleractinian coral *Astrangia poculata* to elevated pCO$_2$ and the
effects of nutrients, zooxanthellae and gender. Biogeosciences 9: 29–39.
doi:10.5194/bg-9-29-2012

Holcomb M, McCorkle DC, Cohen AL (2010) Long-term effects of nutrient and CO$_2$
enrichment on the temperate coral *Astrangia poculata* (Ellis and Solander,1786).
J. Exp. Mar. Biol. Ecol. 386: 27-33.

Holcomb M, Venn AA, Tambutté E, Tambutté S, Allemand D, Trotter J, McCulloch M
(2014) Coral calcifying fluid pH dictates response to ocean
acidification. Scientific Reports 4 (5207):1-4. doi: 10.1038/srep05207

Horwitz R, Borell EM, Yam R, Fine M (2015) Natural high pCO$_2$ increases autotrophy in
Anemonia viridis (Anthozoa) as revealed from stable isotope (C, N) analysis.
Scientific Reports 5 (8779):1-9.

Houlbreque F, Meibom A, Cuif J-P, Stolarski J, Marrocchi J, Ferrier-Page C, Domart-
Coulon I, Dunbar RB (2009) Strontium-86 labeling experiments show spatially
heterogeneous skeletal formation in the scleractinian coral Porites porites.
Geophys. Res. Lett. 36:04604 doi:10.1029/2008GL036782.

Hutchings PA (1986) Biological destruction of coral reefs. Coral Reefs 4:239-252

IPCC (2013): Climate Change 2013: The Physical Science Basis. Contribution of

Working Group I to the Fifth Assessment Report of the Intergovernmental Panel

on Climate Change[Stocker TF, Qin D, Plattner G-K, Tignor M, Allen SK,

Boschung J, Nauels A, Xia Y, Bex V, Midgley PM(eds.)]. Cambridge University

Press, Cambridge, United Kingdom and New York, NY, USA, 1535 pp,

doi:10.1017/CBO9781107415324

Kleypas JA, Buddemeier RW, Archer D, Gattuso J-P, Langdon C, Opdyke BN (1999a)

Geochemical consequences of increased atmospheric carbon dioxide on coral

reefs. Science 284 (5411):118-120. doi: 10.2307/2899149.

Kleypas JA, McManus JW, Meñez LAB (1999b) Environmental limits to coral reef

development: where do I draw the line? American Zoologist 39:146-159.

Kleypas JA, Feely RA, Fabry VJ, Langdon C, Sabine CL, Robbins LL (2006) Impacts of

ocean acidification on coral reefs and other marine calcifiers: A guide for future

research. National Science Foundation, the National Oceanic and Atmospheric

Administration, and the U.S. Geological Survey.

Knoll AH, Bambach RK, Payne JL, Pruss S, Fischer WW (2007) Paleophysiology and

end-Permian mass extinction. Earth and Planetary Science Letters 256:295-313

Knowlton N (2001) Coral Reef Biodiversity-Habitat Size Matters. Science 292:1493

Laborel J (1974) West African reefs corals: an hypothesis on their origin. Proceedings of

the 2nd International Coral Reef Symposium 1: 425–443

LaJeunesse TC (2002) Diversity and community structure of symbiotic dinoflagellates

from Caribbean coral reefs. Marine Biology 141:387-400.

Langdon C, Atkinson MJ (2005) Effect of elevated pCO$_2$ on photosynthesis and

calcification of corals and interactions with seasonal change in

temperature/irradiance and nutrient enrichment. J. Geophys. Res., 110, C09S07, doi: 10.1029/2004JC002576.

Le Quere C, Raupach MR, Canadell JG, Marland G, et al. (2009) Trends in the sources and sinks of carbon dioxide. Nature Geosci 2 (12):831-836.

Leclercq N, Gattuso J-P, Jaubert J (2002) Primary production, respiration, and calcification of a coral reef mesocosm under increased CO_2 partial pressure. Limnol. Oceanogr. 47:558–564

Lewis E, Wallace DWR (1998) Program developed for CO_2 system calculations. ORNL/CDIAC-105. Carbon Dioxide Information Analysis Center, Oak Ridge National Laboratory, US Department of Energy, Oak Ridge, Tennesse.

Lürig M, Kunzmann A (2015) Effects of episodic low aragonite saturation and elevated temperature on the physiology of *Stylophora pistillata*, J. Sea Res. http://dx.doi.org/10.1016/j.seares.2015.01.005

Lüthi D, Le Floch M, Bereiter B, Blunier T, Barnola JM, Siegenthaler U, Raynaud D, Jouzel J, Fischer H, Kawamura K,Stocker TF (2008) High-resolution carbon dioxide concentration record 650,000–800,000 years before present. Nature 453(7193):379-382.

Marubini F, Ferrier-Pagès C, Furla P, Allemand D (2008) Coral calcification responds to seawater acidification: a working hypothesis towards a physiological mechanism. Coral Reefs 27:491-499.

McCulloch M, Falter J, Trotter J, Montagna P (2012) Coral resilience to ocean acidification and global warming through pH up-regulation. Nature Climate Change 2: 623-627.

Meibom A, Cuif J-P, Houlbreque F, Mostefaouia S, Dauphin Y, Meibom KL, Dunbar R (2008) Compositional variations at ultra-structure length scales in coral skeleton. Geochim. Cosmochim. Acta 72:1555-1569.

Mehrbach C, Culberso C, Hawley J, Pytkowic R (1973) Measurement of apparent dissociation constants of carbonic-acid is seawater at atmospheric pressure. Limnol. Oceanogr. 18: 897-907.

Miller AW, Blackwelder PL, Al-Sayegh H, Richardson LL (2011) Fine-structural analysis of black band disease-infected coral reveals boring cyanobacteria and novel bacteria. Dis. Aquat. Organ. 93:179–190.

Miller AW, Richardson LL (2011) Fine structure analysis of black band disease (BBD) infected coral and coral exposed to the BBD toxins microcystin and sulfide. J. Invertebr. Pathol. doi:10.1016/j.jip.2011.09.007

Miller SL, Precht WF, Rutten LM, Chiappone M (2013) Florida Keys Population Abundance Estimates for Nine Coral Species Proposed for Listing Under the U.S. Endangered Species Act. Technical Series Report. Nova Southeastern University Oceanographic Center, Technical Series Report, 1(1). Dania Beach, FL. 85 pp.

Moss RH, Edmonds JA, Hibbard KA, Manning MR, Rose SK, van Vuuren DP, Carter TR, Emori S, Kainuma M, Kram T, Geehl GA, Mitchell JFB, Nakicenovic N, Riahi K, Smith SJ, Stouffer RJ, Thomson AM, Iyant JP, Wilbanks TJ (2010) The next generation of scenarios for climate change research and assessment. Nature 463 (7282):747-756.

Moya A, Huisman L, Ball EE, Hayward DC, Grasso LC, Chua CM, Woo HN, Gattuso J-P, Foret S, Miller DJ (2012) Whole transcriptome analysis of the coral *Acropora millepora* reveals complex response to CO_2-driven acidification during the

initiation of calcification. Molecular Ecology :1-15. doi:10.1111/j.1365-294X.2012.05554.x

Pandolfi JM, Connolly SR, Marshall DJ, Cohen AL (2011) Projecting coral reef futures under global warming and ocean acidification. Science 333(6041): 418-422

Petit J-R, Jouzel J, Raynaud D, Barkov NI, Barnola J-M, Basile I, Bender M, et al. (1999) Climate and atmospheric history of the past 420,000 years from the Vostok ice core, Antarctica. Nature 399(6735): 429-436.

Rahman MA, Oomori T (2010) The role of carbonic anhydrase enzyme in the biocalcification process of coral and its resilience to global climate change. OCEANS 2010 IEEE:1-5. doi:10.1109/OCEANSSYD.2010.5603507

Raven J, Caldeira K, Elderfield H, Hoegh-Guldberg O, Liss P, Riebesell U, Shepherd J, Turley C, Watson A (2005) Ocean acidification due to increasing atmospheric carbon dioxide. London: The Royal Society.

Richardson LL (2004) Black band disease. In: Rosenberg, E., Loya, Y. (Eds.), Coral Health and Disease. Springer, Berlin, 325–336.

Riebesell U, Fabry VJ, Hansson L, Gattuso J-P (eds.) (2010) Guide to best practices for ocean acidification research and data reporting, 260 p. Luxembourg: Publications Office of the European Union.

Ries JB (2011) A physicochemical framework for interpreting the biological calcification response to CO_2-induced ocean acidification. Geochim. Cosmochim. Acta 75:4053-4064.

Ries JB, Cohen AL, McCorkle DC (2010) A non-linear calcification response to CO_2-induced ocean acidification by the coral *Oculina arbuscula*. Coral Reefs 29:661-674.

Ries JB, Cohen AL, McCorkle DC (2009) Marine calcifiers exhibit mixed responses to
  CO_2-induced ocean acidification. Geology 37(12):1131-1134.

Sabine CL, Feely RA, Gruber N, Key RM, Lee K, Bullister JL, Wanninkhof R, Wong
  CS, Wallace DWR, Tilbrook B, Millero FJ, Peng T-H, Kozyr A, Ono T, Rios AF
  (2004) The oceanic sink for anthropogenic CO_2. Science 305:367-371.

Schneider K, Erez J (2006) The effect of carbonate chemistry on calcification and
  photosynthesis in the hermatypic coral *Acropora eurystoma*. Limnol Oceanogr
  51(3):1284–1293.

Schoepf V, Grottoli AG, Warner ME, Cai W, Melman TF, Hoadley KD, Pettay DT, Hu
  X, Li Q, Xu H, Wang Y, Matsui Y, Baumann JH (2013) Coral energy reserves
  and calcification in a high-CO_2 world at two temperatures. PLOS one 8(10):1-11
  e75049.

Silbiger NJ, Donahue MJ (2015) Secondary calcification and dissolution respond
  differently to future ocean conditions. Biogeosciences 12:567-578.

Smith SV, Key GS (1975) Carbon dioxide and metabolism in marine environments.
  Limnology and
  Oceanography 20:493-495.

Sponberg AF (2007) Ocean Acidification: The biggest threat to our oceans? BioScience
  57 (10):822. doi: 10.1641/B571004.

Sterrer W (ed) (1986) Marine fauna and flora of Bermuda. Wiley, New York 774 pp

Strahl J, Stolz I, Uthicke S, Vogel N, Noonan SHC, Fabricius KE (2015) Physiological
  and ecological performance differs in four coral taxa at a volcanic carbon dioxide
  seep. Comparative Biochemistry and Physiology Part A: Molecular & Integrative
  Physiology 184:179-186.

Tambutte E, Venn AA, Holcomb M, Segonds N, Techer N, Zoccola D, Allemand D, Tambutte S (2015) Morphological plasticity of the coral skeleton under CO_2-driven seawater acidification. Nat. Commun. 6:7368 doi: 10.1038/ncomms8368

Towle EK, Enochs IC, Langdon C (2015) Threatened Caribbean Coral Is Able to Mitigate the Adverse Effects of Ocean Acidification on Calcification by Increasing Feeding Rate. PLoS ONE 10(9): e0139398. doi: 10.1371/journal.pone.0139398

Turley C, Blackford JC, Widdicombe S, Lowe D, Nightingale PD, Rees AP (2006) Reviewing the impact of increased atmospheric CO_2 on oceanic pH and the marine ecosystem. In: Schellnhuber H.J, Carmer W, Nakicenovic N, Wigley T, Yohe G (Eds), Avoiding Dangerous Climate Change, 8. Cambridge University Press, Cambridge, pp. 65-70.

Turley C, Eby M, Ridgwell AJ, Schmidt DN, Findlay HS, Brownlee C, Riebesell U, Fabry VJ, Feely RA, Gattuso J-P (2010) The societal challenge of ocean acidification. Marine Pollution Bulletin 60(6): 787-792.

UNEP (2006) Marine and Coastal Ecosystems and Human Well-Being: A Synthesis Report Based on the Findings of the Millennium Ecosystem Assessment. UN Environment Programme, Nairobi.

Uppstrom LR (1974) The boron/chlorinity ratio of the deep-sea water from the Pacific Ocean. Deep-Sea Research I 21:161-162.

Venn A, Tambutté E, Holcomb M, Allemand D, Tambutté S (2011) Live tissue imaging shows reef corals elevate pH under their calcifying tissue relative to seawater. PLoS ONE 6:e20013.

Vernon JEN, Hoegh-Guldberg O, Lento TM, Obura DO, Pearce-Kelly P, Sheppard CRC, Spalding M, Stafford-Smith MG, Rogers AD (2009) The coral reef crisis: The critical importance of <350ppm CO_2. Marine Pollution Bulletin 58:1428-1436.

Wagner DE, Kramer P, van Woesik R (2010) Species composition, habitat, and water quality influence coral bleaching in southern Florida Marine Ecology Progress Series 408:65-78.

Wild C, Hoegh-Guldberg O, Naumann MS, Colombo-Pallota MF, Ateweberhan M, Fitt WK, Iglesias-Prieto R, Palmer C, Bythell JC, Ortiz J-C, Loya Y, van Woesik R (2011) Climage change impedes scleractinian corals as primary reef ecosystem engineers. Marine and Freshwater Research 62:205-2015.